Determining the Cell Size of Yeast Using Diffusion-Weighted NMR

Øyvind Holmås Hardeland

Abstract

This study uses diffusion weighted NMR to determine yeast cell size at different times after those cells were suspended in water. Both the water diffusion and the metabolite diffusion where used in those measurements. Diffusion weighted NMR is a well-studied noninvasive tool that can be used to study various microstructures. Yeast is a cheap and versatile model system for more complex biological systems.

To measure the metabolites they first had to be identified in the NMR spectrum of the yeast cells suspensions. The identification was done by extracting the metabolites from the yeast cells using ethanol. This allowed for identification of several specific metabolite signals, although there was still a lot of overlapping signals in the spectrum that could not be identified.

Dried yeast, of the species Saccharomyces Cerevisiae, was washed and suspended in a 10 % D_2O phosphate buffer. These suspensions were measured using several PFGSE NMR experiments, with varying diffusion times, and with and without water suppression. The data from these measurements were used to determine time dependent diffusion coefficients. Because of the restrictions on the diffusion of molecules due to the cell wall, there is a decline in time dependent diffusion coefficient with increasing diffusion time, and this decline can be used to determine the cell size.

The metabolite measurements of cell size in the yeast samples show apparent growth from around 1,9 μm at 3 days suspended to around 3,5 μm at 12 days suspended. The intracellular water signal did not show this growth, staying around 1,6 μm. These values all fit within a reasonable range of known values for the cell radius of Saccharomyces Cerevisiae yeast, which is between 1,9 and 3,3 μm. [31] The growth in cell size can be attributed to the cells actually swelling, or to the cells dying and the cell walls becoming more permeable. The lack of growth in the water signal means that the water signal is likely less sensitive towards changes in microstructure. This might be because of influence from the extracellular water signal, or because there is less relative change in cell membrane permeability, as water already had comparatively rapid cell membrane exchange, as compared to the metabolites

Cell size was also measured in a layered sample using slice selective measurements. One layer had yeast that had been suspended 12 days and the other had yeast that had been suspended 3 days. The slice selective diffusion measurements gave cell sizes that were larger than the cell sizes from the non-selective measurements, around 4 μm. It is difficult to determine the reason for the larger cell, but a gradient may not have been calibrated correctly at the location that was measured. The slice selective measurements also had larger uncertainties than the non-slice selective measurements. The larger uncertainties was likely from equipment of lower quality or the measurements having different geometry.

Acknowledgements

First, I would like to thank my supervisor, John Georg Seland, for teaching me a lot, for guiding me with his expertise and for being patient when I did not understand something.

I would also like to thank everyone at the department of chemistry at UiB. The teachers for all their help and the students for the good times working and learning together.

Finally, I would like to thank my family and friends for all the support they have shown me throughout my education.

Symbols and Abbreviations

Symbols

P – Angular momentum

I – Angular momentum quantum number

h - Planck's constant

μ – magnetic moment

γ – Gyromagnetic ratio

$\vec{B_0}$ – Static magnetic field

$\vec{B_1}$ – Static magnetic field

$B(r)$ – Magnetic field at position r

$\vec{\omega}$ – Angular frequency

$\vec{\omega}_L$ – The Lamour frequency

$\vec{\omega}(r)$ – The resonance frequency at position r

θ – Flip angle

τ_p – Pulse duration

v – Frequency

σ – Shielding constant

δ – Chemical shift; gradient duration

v_{ref} – Reference frequency for finding chemical shift

$\vec{M}$ – Bulk Magnetization Vector

r – A given coordinate

D – Diffusion

T_1 – Exponential time constant of the spin-lattice relaxation

T_2 – Exponential time constant of the spin-spin relaxation

T_2^* - Total apparent magnetization decay in xy-plane

T_2' – Magnetization decay from dephasing in the xy-plane

A_0 – Initial magnetization constant

G – Gradient amplitude

r – A given coordinate

Φ – Phase shift

t_{dif} – Diffusion time

S – Surface

V – Volume

k - γδg

D(t) – Time dependent diffusion

D_0 – Initial diffusion

$\vartheta(t_{dif})$ – Higher order terms of the time dependent diffuison

R – radius

G_z – Gradient at a position z

$\vec{\omega}_z$ – Resonance frequency at position z

Δz – The thickness of a slice in a slice selective experiment

Abbreviations

NMR – Nuclear Magnetic Resonance

MRI – Magnetic Resonance Imaging

FID – Free Induction Decay

EC – Extracellular

IC – Intracellular

PFGSE – Pulsed Field Gradient Spin Echo

PFGSTE – Pulsed Field Gradient Spin Stimulated Echo

Contents

1 Introduction

1.1 Background

A common method of studying complex organisms, such as humans or other animals, is to study a less complex model system that approximates some aspect of the more complex organism. Samples of these model systems are often cheaper, more environmentally friendly or more ethical to procure and/or produce. Sometimes they are also more adjustable or versatile. One such model system is yeast.

Oxford Concise Medical dictionary defines yeast as "any of a group of fungi in which the body (mycelium) consists of individual cells, which may occur singly, in groups of two or three, or in chains." [1] The spices *Saccharomyces cerevisiae*, which is the one used here, is widely studied and often used as a model system in various sciences. It is well suited for this because of, amongst other things, its rapid growth, dispersed cells, well defined genetic system and versatile DNA transformation system. It is also nonpathogenic and readily available. [2]

NMR is a set of spectroscopy techniques first described by Bloch et.al. [3] and Purcell et.al. [4] in 1946. It has a wide set of applications within chemistry and physics, and the imaging techniques that are derived from it, MRI, are particularly useful as a research and non-invasive diagnostic tool in medicine. In this study, NMR is used as a spectroscopy tool, and as a tool for measuring diffusion.

1.2 Goals of the study

The main goal of the study is to examine whether cell size can be determined from the restricted diffusion of its metabolites, in a yeast model system. Being able to find the structural properties of cells, e.g. the cell radius, could be especially useful in the field of medicine. For example Helmer et. al. found that structural changes tumor tissue could be measured through measuring their cell size. This could be to measure the progress in tumor treatments. [5]

The cell size will be determined through NMR spectroscopy, specifically diffusion measurements using pulse field gradients. To accomplish this the metabolites must be identified in a NMR spectrum, and this will be done by extracting the metabolites from the cells.

Furthermore, the study will try to examine the effect of time on the yeast suspensions, specifically whether being suspended for any length of time impacts the cell size. That goal will both be pursued by measuring in sample of different ages, and by measuring specific volumes in one sample with differently aged yeast.

Finally, the study also seeks to determine whether the metabolites exist outside the cell structure in a yeast suspension. If it does, this could influence the results of the main goal. To determine whether the metabolites has an extracellular (EC) component, a metabolites diffusion will be measured at different yeast to water ratios. Then, these measurements will be solved for two components, and the intensity of those components will be compared for each measurement.

1.3 Former work

Using NMR diffusion measurements to study various microstructures, has a nearly thirty year history. Mitra et.al measured the structure of porous media using water diffusion in their studies from 1992 and 1993 [6-7]. Most of the later work is based on the techniques from those articles.

Hürlimann et.al measured diffusion in sandstone core, and used that to find properties of its geometry in their 1994 study. [8]

It was quickly realized that these techniques could be used to examine microstructure in biological systems. In 1994, Latour et.al used the diffusion propagator to measure the changes in packed erythrocytes after ischemia occurred in the brain. [9]

A year later, Helmer et. al. used the technique to examine the changes in microstructure between necrotic and non-necrotic tumor tissue. [5] All the articles mentioned measured water diffusion. Later studies would start measuring the diffusion of metabolites.

By now, a wide variety of applications for these techniques have been found. As explained in an overview article by Ronen et.al [10], measuring metabolite diffusion in vivo began with ^{31}P diffusion-weighted measurements in skeletal muscle. There were many discoveries from this work, amongst them that metabolite diffusion along muscle fibers is close to free, meaning metabolites are not confined to subcellular organelles.

The article by Ronen et.al [10] explains further about diffusion-weighted metabolite studies on the brain. Those studies could use ^{1}H measurements, as the spectral quality is better in the brain than in the skeletal muscle. Those studies did, for example, measure microstructural properties in the brain cells, approximate the viscosity of brain cell cytosol and determine differences in metabolite apparent diffusion coefficients between gray and white matter in the brain.

Diffusion weighted NMR measurements also have applications towards specific diseases. In addition to the applications for cerebral ischemia and cerebral tumors mentioned above, diffusion-weighted NMR could have application towards studying aging, and neurodegenerative and psychiatric diseases. [10]

As mentioned in the background, yeast is an often-studied model system, and is used in chemistry, biology and medicine. There are even many articles using yeast that are related specifically to diffusion and microstructure. For example studies of cell membrane water exchange with [11] or without relaxation weighting effects [12]. Diffusion weighing has also been combined with relaxation weighing to measure compartmental diffusion coefficients [13]

Alrodi et.al developed a method for extracting metabolites from yeast cells, which was used here. [14]

2 Theory

2.1 NMR

NMR is a type of spectroscopy. The basis of its methods is a property of atomic nuclei called spin. The nuclei's spin gives them angular momentum, P, which is defined by equation 2.1.1

$$P = \sqrt{I(I + 1)}\hbar$$
Equation 2.1.1

I is the angular momentum quantum number, also called nuclear spin, and can be any multiple of ½ with a value between 0 and 6, while $\hbar = h/2\pi$ where h is Planck's constant. The magnetic moment μ is defined by equation 2.1.2, where γ is the gyromagnetic ratio. This is a constant relating to each different nuclei and their spin, and a higher γ gives a stronger signal in NMR.

$$\mu = \gamma P$$
Equation 2.1.2

It follows that nuclei with I equal zero also has no magnetic moment, and are not observable in an NMR spectrum. This can lead to a signal-intensity problem with nuclei where the most abundant isotope has no angular momentum. This is the case for ^{12}C, which is the most abundant isotope of carbon (98,9 %). When carbon is used in NMR experiments the isotope measured is ^{13}C (1,07 % abundance), which means only a hundredth of the nuclei have the ability to contribute to the signal. For this study only hydrogen atoms have been measured, where the most abundant nuclei is ^{1}H (99,99 %) and so almost all the nuclei have the possibility of contributing to the signal.

To receive any signal in NMR the measurable nuclei must be placed in a magnetic field, $\overrightarrow{B_0}$. The magnetic moment is now time dependent as shown by equation 2.1.3. The coordinate system is defined as the z-axis being along the direction of $\overrightarrow{B_0}$.

$$\frac{d\vec{\mu}}{dt} = \vec{\mu} \times \gamma\overrightarrow{B_0}$$
Equation 2.1.3

To solve the above equation a rotating frame of reference will be used. In the rotating frame of reference the xy-plane rotates at an angular frequency $\vec{\omega}$. This transforms equation 2.1.3 into equation 2.1.4.

$$\frac{d\vec{\mu}}{dt} = \vec{\mu} \times \left(\gamma\overrightarrow{B_0} + \vec{\omega}\right)$$
Equation 2.1.4

If $\vec{\omega} = -\gamma B_0$ then $\frac{d\vec{\mu}}{dt} = 0$. This means that the angular momentum is static in the rotating coordinate system. Also, in the laboratory frame the angular momentum is rotating at the Lamour frequency $\overrightarrow{\omega_L}$, which is given by equation 2.1.5.

$$\overrightarrow{\omega_L} = -\gamma B_0$$
Equation 2.1.5

When an electromagnetic (RF) pulse, which has a magnetic field $\overrightarrow{B_1}$, is applied orthogonally to the z-axis, the angular momentum also becomes time dependent as given by equation 2.1.6. The angular momentum of the spins can now be described as rotating towards the xy-plane.

$$\frac{d\vec{\mu}}{dt} = \vec{\mu} \times \gamma\overrightarrow{B_1}$$
Equation 2.1.6

From equation 2.1.5 it can be shown that when $\overrightarrow{B_1}$ is applied along the x-axis the $\vec{\mu}$ will rotate in the yz-plane at an angular frequency given by equation 2.1.7.

$$\vec{\omega_1} = \gamma B_1 \qquad\qquad \text{Equation 2.1.7}$$

The flip angle, θ, is the angle that the angular momentum will be shifted and is given by equation 2.1.8. τ_p is the duration of the pulse.

$$\theta = \gamma B_1 \tau_p \qquad\qquad \text{Equation 2.1.8}$$

Because of the rotating frame of reference $\vec{\mu}$ will appear static in the xy-plane when $\vec{B_1}$ is turned off, but it does still precess at $\vec{\omega_L}$. This precession will generate a current in a coil that surrounds the sample, which the computer registers as a signal. The signal is received as a free induction decay (FID).

A Fourier transform of the FID gives a spectrum which plots signal intensity against signal. The signal frequency is given by equation 2.1.9. σ is the shielding constant of the nuclei. It is this variable allows for differentiation between different nuclei of the same element in a sample, because there will be small differences in their magnetic field. These differences come from the electrons that binds the atoms together.

$$\nu = \frac{\gamma B_0 (1-\sigma)}{2\pi} \qquad\qquad \text{Equation 2.1.9}$$

Because the above equation is dependent on B_0 and there is difference in B_0 from one NMR instrument to another, chemical shift, δ, is normaly used instead of frequency. Chemical shift is defined by equation 2.1.10, and is quoted as part per million, ppm. ν_{ref} is a reference frequency, the resonance frequency of TMS.

$$\delta = 10^6 \times \frac{\nu - \nu_{ref}}{\nu_{ref}} \qquad\qquad \text{Equation 2.1.10}$$

There is only a small surplus of the angular momentums that will be aligned with B_0. This surplus means that at equilibrium there will be a positive net magnetization vector. That macroscopic magnetization is given by equation 2.1.11.

$$\vec{M} = \sum \vec{\mu} \qquad\qquad \text{Equation 2.1.11}$$

Before the B_1 field is applied $\vec{M}$ will have no xy component since the rotation of the angular momentums are out of phase. After the RF pulse $\vec{M}$ is time dependent as described in equation 2.1.12. This is means that it rotates to the rotating xy-plane in the same way that the spin do, as described in equation 2.1.8.

$$\frac{d\vec{M}}{dt} = \vec{M} \times \gamma \vec{B_1} \qquad\qquad \text{Equation 2.1.12}$$

[15-17]

2.2 Diffusion

As particles in a suspension or in other colloidal systems move through their medium they will be constantly changing direction. This comes from collisions with the molecules in the medium, and is called Brownian motion. For spherical particles such as cells this leads to diffusion, which is the net movement of the particles. The Brownian displacement, $(r - r')$, can be described by equation 2.2.1, where t is time and D is the diffusion coefficient. [18]

$$(r - r') = \sqrt{2Dt} \qquad\qquad \text{Equation 2.2.1}$$

Large and heavy molecules usually move slower that smaller and lighter ones.

2.3 Yeast cells

Fungi are simple eukaryotes, like plants and animals, but unlike bacteria, which are prokaryotes. This means that they have a nucleus where their DNA is stored. Yeast separates from other fungi in that they are single celled lifeforms, though they can occur in small groups or chains.

Figure 2.3.1: Cross section of a yeast cell [19]. V is the vacuole, which is the yeast cells largest organelle and is involved in trafficking proteins intracellularly. N is the nucleus where the chromosomes are. M points to the mitochondria, this is where energy is generated in the form of ATP using oxygen and glucose. These organelles are located in the cytoplasm. PM is the plasma membrane, a phospholipid bilayer which controls the permeability of this cell, i.e. it controls what can and can't enter or exit the cell. CW is the cell wall, which protects the inner structure and gives the cell firmness. It is rigid, with an outer layer of mannan and an inner layer of glucan fibrosis.

2.4 Relaxation and the spin echo experiment

When magnetization precesses in the transverse plane it will slowly return to its equilibrium along the z-axis. That decay of magnetization is called relaxation. Relaxation happens both by the magnetization returning to the z-axis, with an exponential time constant T_1, and by it declining in along the x- and y-axis, with an exponential time constant T_2. Their macroscopic effect on the magnetization are described in the Bloch equations below. M_0 refers to the magnetization at equilibrium. [16]

$$\frac{dM_z}{dt} = -\frac{M_0 - M_z}{T_1}$$
Equation 2.4.1

$$\frac{dM'_x}{dt} = -\frac{M'_x}{T_2}$$
Equation 2.4.2

$$\frac{dM'_y}{dt} = -\frac{M'_y}{T_2}$$
Equation 2.4.3

Equation 2.4.1. can be solved to give equation 2.4.X, which gives the z-magnetization after a RF-pulse. A_0 is a constant dependent on the initial magnetization. Right after a 90° pulse there will be no z-magnetization, in which case A_0 will be 1.

$$M_z = M_0 \left(1 - A_0 e^{-\frac{t}{T_1}}\right)$$
Equation 2.4.X

The transverse magnetization also decays because inhomogeneities in the magnetic field dephases the magnetization. This means that the xy- magnetization is given in equation 2.4.4. T_2^* is the total apparent decay of the transverse magnetization, and is given by equation 2.4.5, in which T_2' is the apparent decay caused by the additional dephasing.

$$M_{xy} = M_0 e^{-\frac{t}{T_2^*}}$$
Equation 2.4.4

$$\frac{1}{T_2^*} = \frac{1}{T_2} + \frac{1}{T_2'}$$
Equation 2.4.5

The T_2' decay can be refocused using a spin echo pulse sequence, shown below.

$$90_x^o \rightarrow \tau \rightarrow 180_x^o \rightarrow \tau \rightarrow \text{FID}$$

90°x refers to a 90° pulse from the direction of the x-axis while τ refers to a time interval.

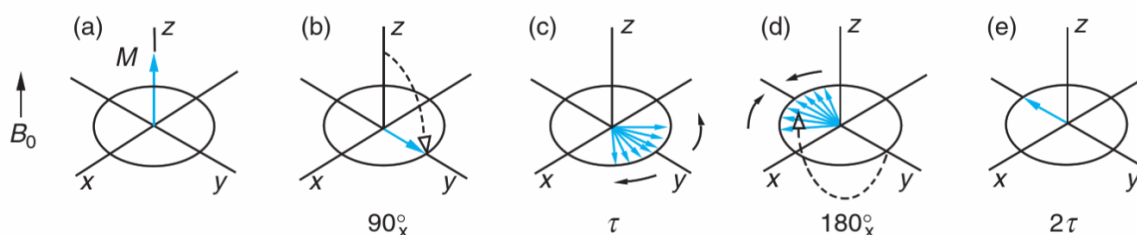

Figure 2.4.1: Shows how the magnetization behaves during a spin echo sequence. First the 90°x pulse flips the magnetization into the xy-plane. After τ the inhomogeneities in the magnetic field have caused the magnetization to dephase. The 180°x pulse flips the magnetization, but not the way the magnetization dephasing is moving. Since the time interval after the 180°x pulse is equal to the time interval after that pulse, the magnetization will rephase as much as it dephased, and be refocused. Adapted from [16]

2.5 Determining diffusion using pulse field gradient spin echo (PFGSE) NMR

Diffusion is measured by examining its effect on a system's signal in an magnetic field with a controlled inhomogeneity. In such a system diffusion will cause a reduction in the received signal. This is because there will be dephasing of the transverse magnetization as the nuclei move, and the amount of dephasing is dependent on the amount of diffusion. [20]

Controlled inhomogeneity can be induced using a magnetic field gradient. Applying such a gradient causes a strength change in the magnetic field, B(r), such that at a given coordinate, r, it will now be given by equation 2.5.1. It becomes a combination of the normally applied magnetic field, B_0, and the amplitude of the pulsed field gradient, G, multiplied with the coordinate. [21]

$$B(r) = B_0 + G \cdot r$$
Equation 2.5.1

This means that the Lamour frequency of the spins, as given by equation 2.1.8, will vary along the direction of the applied gradient. The new resonance condition is given by equation 2.5.2. $\omega(r)$ is the Lamour frequency of a spin at position r.

$$\omega(r) = -\gamma(B_0 + G \cdot r)$$ Equation 2.5.2

When gradients are applied as pulses, they induce a phase-shift in the transverse magnetization, Φ, as given by equation 2.5.3. [24]

$$\Phi = \gamma\delta gr$$ Equation 2.5.3

When the magnetization is out of phase with the rotating coordinate system, less signal will be received. An important element of this equation is that Φ is dependent on the position of the spins on the z-axis, r. The δ is the duration of the gradient pulse and g is the strength of the gradient.
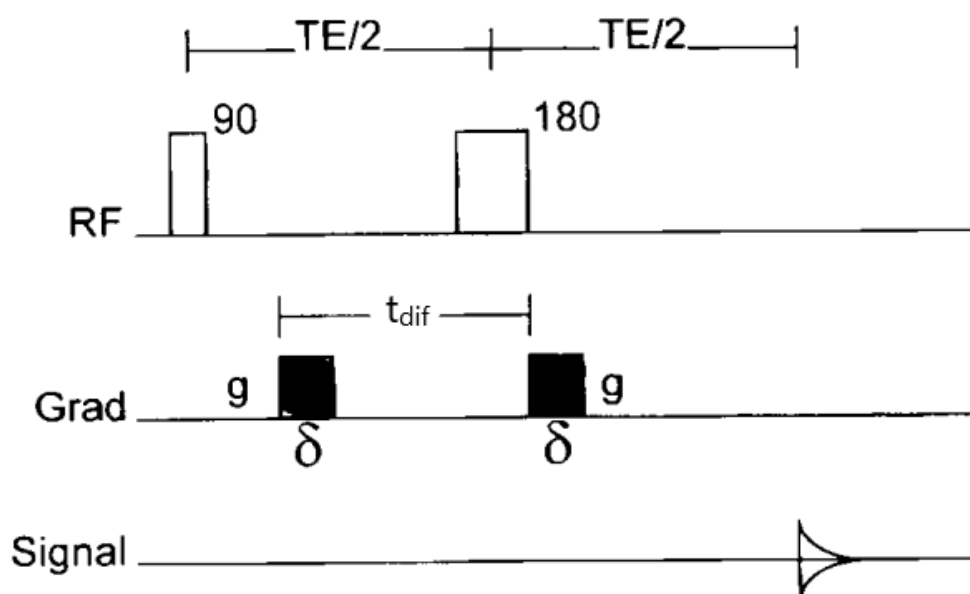
Figure 2.5.X: The simplest form of a PFGSE pulse program. It starts with a 90° RF excitation pulse, followed by a first gradient. Then there is a 180° refocusing pulse, which is followed by another gradient equal to the first. TE is the experiment time, while t_{dif} is the diffusion time, the time from the start of the first gradient to the next. Adapted from [5]

The first gradient pulse dephases the spins according to equation 2.5.3. . If there is no movement, then the 180° pulse and the second gradient refocuses all that dephasing. Because the gradient dephasing is dependent on position, equation 2.5.3 tells us that any movement will lead to a difference in the dephased and the rephased magnetization, ΔΦ. That difference is given by equation 2.5.4.

$$\Delta\Phi = \gamma\delta g(r - r')$$ Equation 2.5.4

The displacement, (r-r'), is the difference of the positions at the first and second gradient, which in bulk equals the average Brownian displacement. Equation 2.2.1 shows that ΔΦ is dependent on diffusion. It does not matter whether ΔΦ is positive or negative, as either means the spins are out of phase with the Lamour frequency, which will reduce the signal.

It can be shown that the magnetization at the end of the PFGSE program is given by equation 2.5.5 [20, 23] where M_0 is the equilibrium magnetization and $k = \gamma g \delta$.

$$M(k,t) = M_0 e^{-k^2 t_{dif} D}$$
Equation 2.5.5

If $\ln(M/M_0)$ is plotted against k^2, with a constant t_{dif}, one can determine the diffusion coefficient D.

2.6 Restricted diffusion and determination of the cell size

Restricted diffusion occurs when there is something restricting the movement of the particles, e.g. the wall of a cell restricting the movement of the molecules inside that cell. Restricted diffusion makes the diffusion coefficient time dependent, as more time means an increased possibility of encountering a restriction.

The time dependent diffusion inside a cell, D(t), is given by equation 2.6.1. [6] S is the surface of the cell and V is the volume. The last term, $\vartheta(t_{dif})$, contains higher order terms that are dependent on t, and can therefore be neglected for short values of t. For longer values of t the higher order terms become relevant, and a different equation would be needed.

$$\frac{D(t)}{D_0} = 1 - \frac{4}{9\sqrt{\pi}} \frac{S}{V} \sqrt{D_0 t_{dif}} + \vartheta(t_{dif})$$
Equation 2.6.1

This also gives the following equation for the surface to volume ratio. This means that this ratio can be found by varying the diffusion time, and plotting the measured diffusion coefficient against the square root of t_{dif}. The $-\partial D(t)/\partial \sqrt{t_{dif}}$ term is the slope of a linear regression of that plot. The initial diffusion coefficient, D_0, is the diffusion when there is no restrictions and can be found through extrapolation to $t_{dif}=0$.

$$\frac{S}{V} = -\frac{\partial D(t)}{\partial \sqrt{t_{dif}}} \frac{9\sqrt{\pi}}{4D_0^{3/2}}$$
Equation 2.6.2

Assuming a spherical cell structure, the radius of the cell, R, is given by equation 2.6.3.

$$R = \frac{3}{\left(\frac{S}{V}\right)}$$
Equation 2.6.3

[source]

For a time dependent diffusion coefficient, equation 2.5.5 can be rewritten as equation 2.6.4.

$$M(k,t) = M_0(t) e^{-k^2 D(t) t_{dif}}$$
Equation 2.6.4

At higher values of k, the above equation will start to deviate from Gaussian behavior. [5] This is because the molecules are affected by the restricting environment during the gradient pulses. As gradient duration is an element of k, the effect becomes stronger for higher values of k. This means that we can only extract an accurate time dependent diffusion coefficient with the initial slope of the $\ln(M/M_0)$ vs. k^2 curve.

The M_0 is now time dependent due to relaxation weighing effects. As the diffusion time is increased, so is inevitably the experiment time. At increased experiment times, T_2 could eventually be influential, which will cause less transverse magnetization. The increased experiment times could therefore have an effect on the results if T_2 is different for the EC and IC component of the water signal, since there is exchange between the EC and the IC water.

There is likely a difference, as Eriksson et.al found in their study that the EC water had a T_2 of 35 to 52 ms, while the IC component had one of 16,1 to 18,1 ms, all depending in yeast strain and temperature. [11] However, since the longest diffusion time in these experiments is 15 ms, such a difference in T_2 is unlikely to have a significant effect.

2.7 Frequency selective pulses

There are three commonly used types of RF pulses in contemporary NMR. Hard pulses are used when there is no need for any selection. They excite a broad range of frequencies, and their lengths are in the order of microseconds. To excite a narrow range of frequencies, either a sinc or a Gaussian pulse, collectively called soft pulses, is applied. The names refer to the shapes of the pulses. These pulses are longer, in the range of hundreds of microseconds to milliseconds, but less intense. [25-27]

The number of protons contributing to a signal is proportional to area of the signal in the ^{1}H NMR spectrum. This can lead to problems if a solvent has a lot of ^{1}H, as its signal will dominate the spectrum and interfere with the signals from the more interesting but less plentiful chemicals. This can sometimes be avoided by using deuterated solvents, but these are more expensive and can sometimes exchange deuterated chemical groups with the solute. Another solution is to saturate the solvent signal with a soft pulse, which will suppress that signal during NMR measurement. [28] An article by Zheng et.al describe the most used solvent suppression techniques. [29]

2.8 Finding cell size using intracellular (IC) water

As diffusion is affected by restriction of movement, extracellular (EC) and IC water will have different diffusion. Therefore, the measured diffusion of the water signal in a yeast cell suspension will have two components, in addition to being affected by the restriction as discussed in 2.6. Since the intracellular component will be the slower one, the initial curve of the $\ln(M/M_0)$ vs. k^2 plot can not be used to find the time dependent diffusion. Instead the plot is fitted and solved for two components, and the slower components are used. Because of the problems with using the higher values of k in the $\ln(M/M_0)$ vs. k^2 explained in section 2.6, this should theoretically mean that measuring the metabolites is more accurate than the water signal.

Another factor that could possibly influence the water diffusion measurements is that there is exchange between the EC and IC water, because water is able to permeate the cell plasma wall. Water has an intracellular lifetime of 0,35 s to 1,0 s when ranging in temperature from 32 ^{o}C to 5 ^{o}C. As the diffusion times are in the order of milliseconds, with a maximum of 15 ms, the exchange should have little effect. [12]

2.9 Slice selective measurements

When there are differences within a sample it can be useful to examine the NMR signal of a small volume within that sample. Examples of this range in complexity from organic tissue, where there is molecular structures, to samples that include different phases. In NMR, this can be done through slice selective excitation.

The goal of slice selection is to be able to measure only a certain volume of a sample. This is accomplished using a slice selective gradient G_z and frequency selective excitation. Using a gradient changes the resonance condition to be spatially dependent as expressed by equation 2.5.2. Rewriting that equation as being specifically along the z-axis gives equation 2.8.1, where z is a given position along the z-axis. [15]

$$\omega_z = -\gamma(B_0 + G_z z) \hspace{4cm} \text{Equation 2.9.1}$$

Combining this with equation 2.1.4, the definition of the Lamour frequency, gives the below equation. It shows how the resonance frequency at position z deviates from the Lamour frequency.

$$\omega_z = \omega_L - \gamma G_z z \hspace{4cm} \text{Equation 2.9.2}$$

The slice selected for has a thickness Δz. The bandwidth of frequencies selected for is then given by equation 2.8.3. Only frequencies within this spatial slice contribute to the NMR signal.

$$\Delta\omega_z = -\gamma G_z \Delta z \hspace{4cm} \text{Equation 2.9.3}$$

The slice thickness can be adjusted by adjusting the bandwidth of frequencies selected for, and the middle position of the slice can be adjusted by adjusting the middle point of the frequency bandwidth.

Slice selection is commonly the first step of Magnetic Resonance Imaging (MRI). MRI is a set of techniques that expands NMR into being capable three-dimensional imaging. By using gradients to mark protons along each axis, the positions of the protons can be mapped out. The data from those measurements can be presented as an image. [20]

3 Experimental

3.1 Preparation of yeast suspensions

Dry yeast from Idun®, of the spices Saccharomyces Cerevisiae, was suspended in water and left overnight, to let gas production occur. The yeast was then washed four times. This was done by centrifuging the yeast down and then removing the water layer that formed on top of it. New distilled water was added and the yeast was vortexed until fully resuspended. After the fourth centrifugation the yeast was suspended in pre-prepared 10% D_2O phosphate buffer (7,4 pH) and this suspension was transferred to a 5 mm NMR-tube.

Four such samples were prepared, numbered 1 through 5, because 3 and 4 are the same sample measured at different times. The samples were left suspended 3, 5, 4, 11 and 12 days respectively. Only the metabolites were measured for sample 1, and only the water signal was measured for sample 2.

3.2 Preparation of yeast extracts

Yeast suspensions were prepared and washed using the same procedure as for yeast suspensions. Afterwards the washed yeast was resuspended in 96% ethanol from the Department of Chemistry by shaking with a vortex for 12x30s. The ethanol layer was separated from the cell remains by 5 min of centrifugation. The ethanol was then dried away in a heating cabinet at 323 K, leaving the dry extract. The sample was then rehydrated with 10 % D_2O phosphate buffer (7,4 pH), and 0,6 mL of this was transferred to a NMR tube. This method of metabolite extraction is based on the method in Alroldi et.al [14], though in that method the cells were kept frozen, which was not done in this case.

3.3 Preparation of samples for testing a metabolite for an EC component

Accurate diffusion measurements of metabolites depend on there being little to no EC component of those metabolites. To test this yeast suspensions were prepared and washed as in section 3.1, and added to a 5 mm NMR-tube. Instead of removing excess water before measurement the sample was shaken so the yeast was evenly distributed across the sample tube.

Diffusion was measured repeatedly with constant diffusion time (10 ms) using a PFGSE pulse sequence, over about 20 hours, during which time some water would rise and some yeast would set. This would mean that a potential extracellular component would contribute less to the signal, as it would rise out of the sampled area with the water.

3.4 Sample preparation for slice selective experiments

Yeast suspensions were prepared and washed as in section 3.1, but then added to a 10mm sample tube. A week later a new sample was prepared and washed. After removing excess water, the newer sample was layered on top of the older, in the same sample tube.

3.5 Measurement details

The metabolites where measured using a PFGSE pulse sequence with pre-saturation of the water signal used as water suppression. There were 16 gradient steps, ranging from 0,65 to 12,90 T/m. The pulse sequence gradient duration was 1,57 ms. The time dependent diffusions of the metabolites were measured with diffusion times ranging from 4 to 15 ms, with 1 ms intervals.

The water was measured using a PFGSE pulse sequence for short diffusion times (4-5 ms) and a 13-interval Pulsed Field Gradient Spin Stimulated Echo (PFGSTE) for longer diffusion times (6-15 ms). There were 32 gradient steps in the PFGSE pulse sequence, ranging from 0,10 to 12,89 T/m. There were 32 gradient steps in the 13-interval PFGSTE pulse sequence, ranging from 0,10 to 12,82 T/m. The pulse sequence gradient duration was 1,57 ms in both cases. The time dependent diffusions of the water was measured with diffusion times ranging from 4 to 15 ms, with 1 ms intervals. All non-selective measurements used a 10 μs excitation pulse.

The 13-interval PFGSTE pulse sequence is shown in figure 3.5.1.
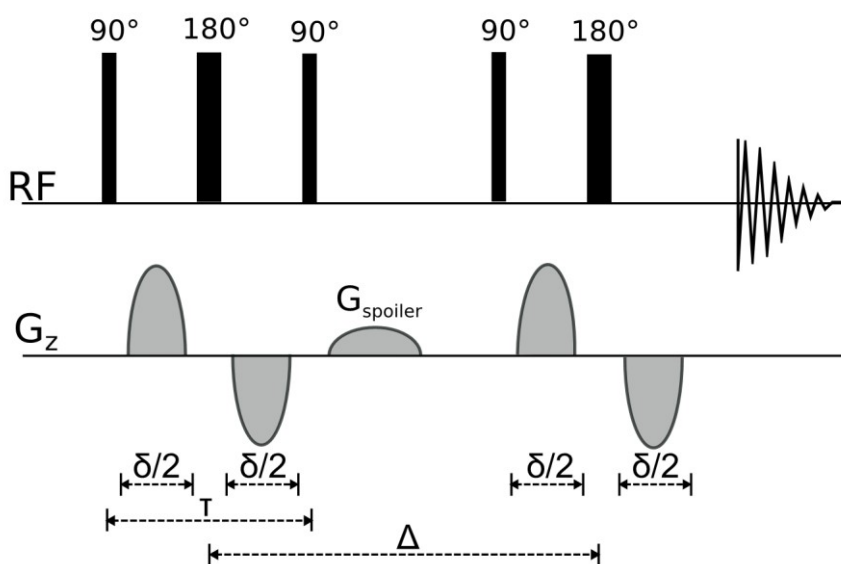
Figure 3.5.1 The 13-interval PFGSTE pulse sequence. The δ is the effective duration of the gradient pulses. Δ is the diffusion time in this figure. T is the time between the first two 90° pulses. This sequence is used to remove the dephasing effects of internal gradients in the sample, and does this via two 180° pulses. Because of the 180° pulse, the gradients of opposite signs that enclose it enhance each other's effect rather than negate each other. $G_{spoiler}$, which is a spoiler gradient, removes the coherent magnetization generated during the evolution period. [30, 31] Figure from [32].

For the slice selective experiments a PFGSE pulse sequence was used to measure the water signal and the metabolite signals 3 mm below and 3 mm above the center of the sample. The sample was placed such that the border between the two layers was the center. There were 16 gradient steps in the PFGSE pulse sequence, ranging from 0,07 to 1,48 T/m. The pulse sequence gradient duration was 1,57 ms. The time dependent diffusions were measured with diffusion times ranging from 3,5 to 14,5 ms, with 1 ms intervals. The slice selective measurements used excitation pulses that were 40 μs long. The pulse sequence of the slice selective measurements are shown in figure 3.5.2.
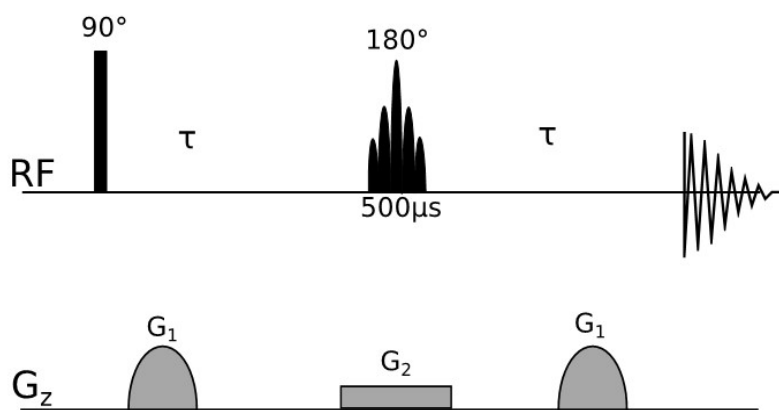
Figure 3.5.2 The slice selective PFGSE pulse sequence. The G_1 gradients are the same as for the regular PFGSE sequence, while the G_2 gradient is the slice selective gradient. The Experiment time is 2τ, and the diffusion time is the time from the start of the first G_1 to the second G_1. Figure from [32].

3.6 Instrument details

All the NMR experiments were performed on a Bruker Ascend 500 WB MHz NMR spectrometer. The nonselective measurements where performed using a Bruker DiffBB broadband gradient probe, while the selective measurements where performed using commercial Bruker MicWB40 micro imaging probe head in combination with the Micro 2.5 gradient system. All experiments where performed at 298 K.

4 Results and Discussion

4.1 Yeast cell extracts

To measure the diffusion of the metabolites, the metabolites must first be identified in the yeast suspension spectrum. To accomplish this, the metabolites were extracted from the yeast using a method presented in an article by Alrodi et.al. [Alrodi]. The spectrum taken from this extract have sharper and less overlapping peaks than the suspension spectrum, which makes the metabolites much easier to identify.
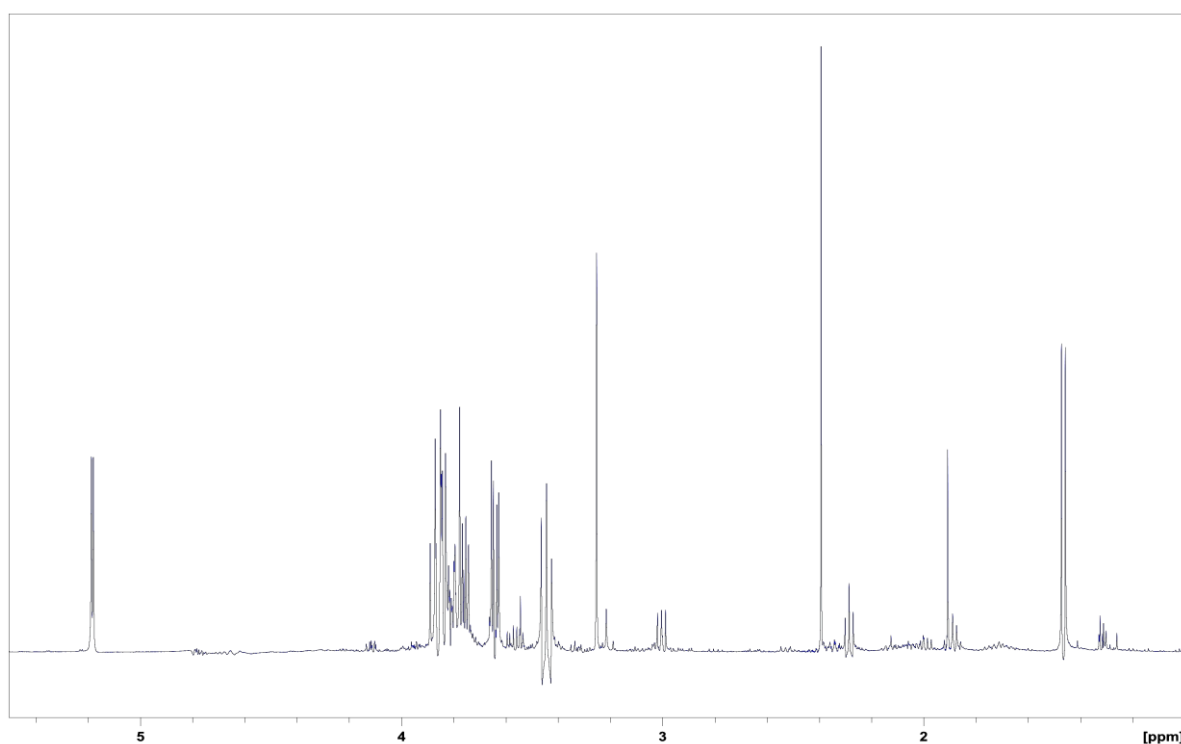
Figure 4.1.1: Yeast cell extraction water suppressed spectrum from 5,5-1,0 ppm.
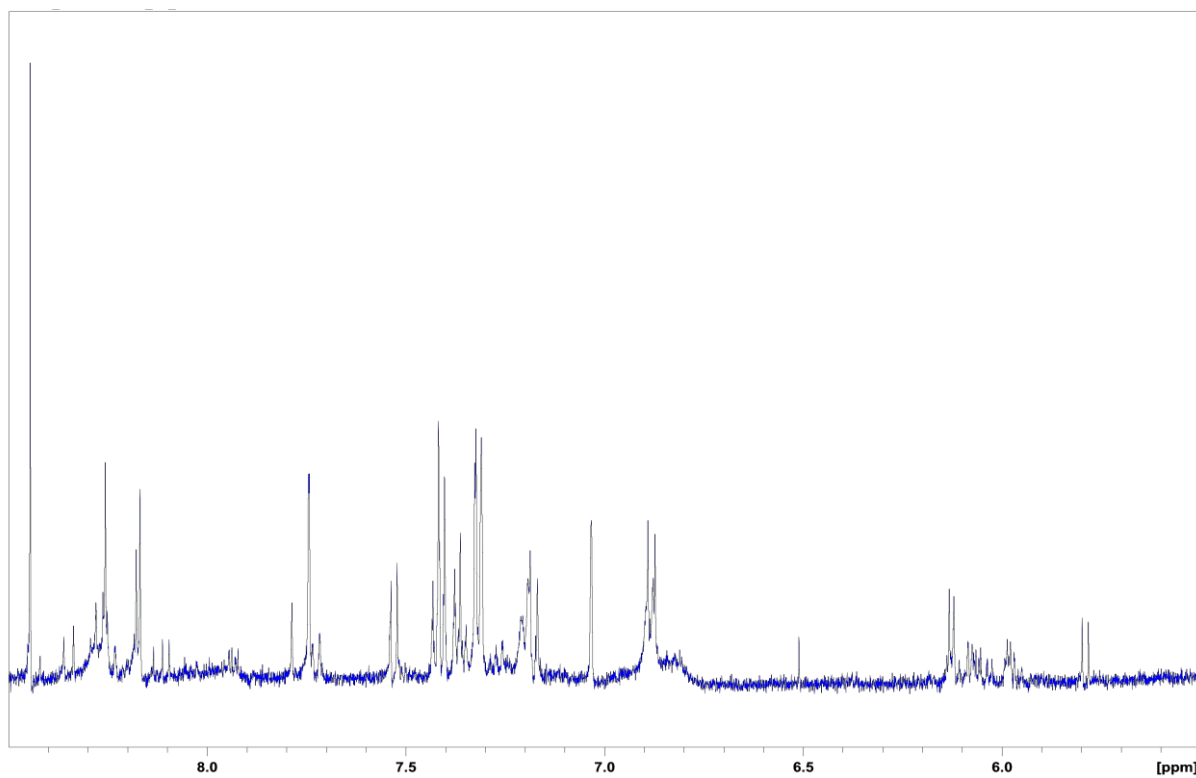
Figure 4.1.2: Yeast cell water suppressed extraction spectrum from 9,0-5,5 ppm.

Figure 4.1.1 and figure 4.1.2 show the spectrum of the yeast extract. There are a lot of different signals, so to identify the metabolites, this spectrum was compared to the study by Alrodi et.al, as shown in table 4.1.1.

Table 4.1.1: Alrodi et.al. [14] identified the below metabolites in their yeast extracts. This table compares those result with the ones found here. Some signals were found, some were less clear and some were apparently not there. The signals in bold were used in the diffusion measurements.

Metabolite	Found signal	Overlapping/weak signal	Missing/Low signal
NAD	9.33 (s) 8.42 (s) 6,13 (d) 6.08 (d) 6.03 (d)	8.19(m)	9.15 (dd) 8.83 (d)
AMP derivative		8.17 (s)	8.6 (s)
UDP derivative		8.94 (d)	
Histidine	7.79 (s) 7.04 (s)	3,96 (dd) 3.22 (dd) 3.12 (dd)	
Phenylanine	7.32 (d)	7.42 (m) 7.36 (m) 3.97 (dd) 3.29 (dd) 3.12 (dd)	
Tyrosine		7.18 (d) 6.89 (d) 3.97 (dd) 3.13 (dd) 3.02 (dd)	
Trehalose	5.18 (d) **3.44** (t)	3.85 (m) 3.75 (dd) 3.64 (dd)	
Lactate	4.11 (dd)	1.32 (d)	
Serien		3.94 (m) 3.83 (dd)	
Glyserol	3.65 (dd)	3.77 (m) 3.55 (dd)	
Glycerophosphocholine	**3.25 (s)**	4.31 (m) 3.6 (dd)	
Lysine	**3 (t)** 1.9 (m) **1.71 (m)**	3.7 (m) 1.45 (m)	3.7 (m)
Citrate	2.65 (d)	2.52 (d)	
Succinate		2.39 (s)	
Glutamate	2.34 (td) 2.05 (m)	3.74 (dd)	
Alanine	**1.47 (d)**		
Valine	1.03 (d)		0,98 (d)
Isoleucine		1 (d)	0,94 (t)
Formate	8.44 (s)		
Uracil	7.53 (d) 5.79 (d)		
Fumarate	6.5 (s)		
Uracil-6-caboxylate			6.18 (s)
Thamine derivate		5.46 (s)/(d)	
Pyruvate		2.36 (s)	
Methionie		2.12 (s)	2.63 (t)
Acetate	1.91 (s)		
Ethaonl		3.65 (q)	1.71 (m)
Asparatate	2.80 (dd)	3.88 (dd)	
Leucine	1.69 (m)	3.71 (m)	0.95 (t)
Glucose	5.22 (d) 3.51 (dd) 3.40 (td)	4.64 (w) 3.89 (dd) 3.83 (m) 3.73 (m) 3.46 (m) 3.23 (dd)	
Threonine			4.24 (m) 1.31 (d)
Phenylacetate			7.38 (m) 7.30 (m) 3.52 (s)
Glutathione ox		3.30 (dd) 2.96 (dd)	

This method of extracting the metabolites from yeast cells, adapted from the one presented in Airoldi et. al [14], seems to work well here. That study used grown yeast cells, as opposed to the dried and resuspended ones used here. That allowed for separating between an exponential and an stationary phase, making it easier to identify individual signals. In the current study there were a lot of overlapping signals that could not be identified.
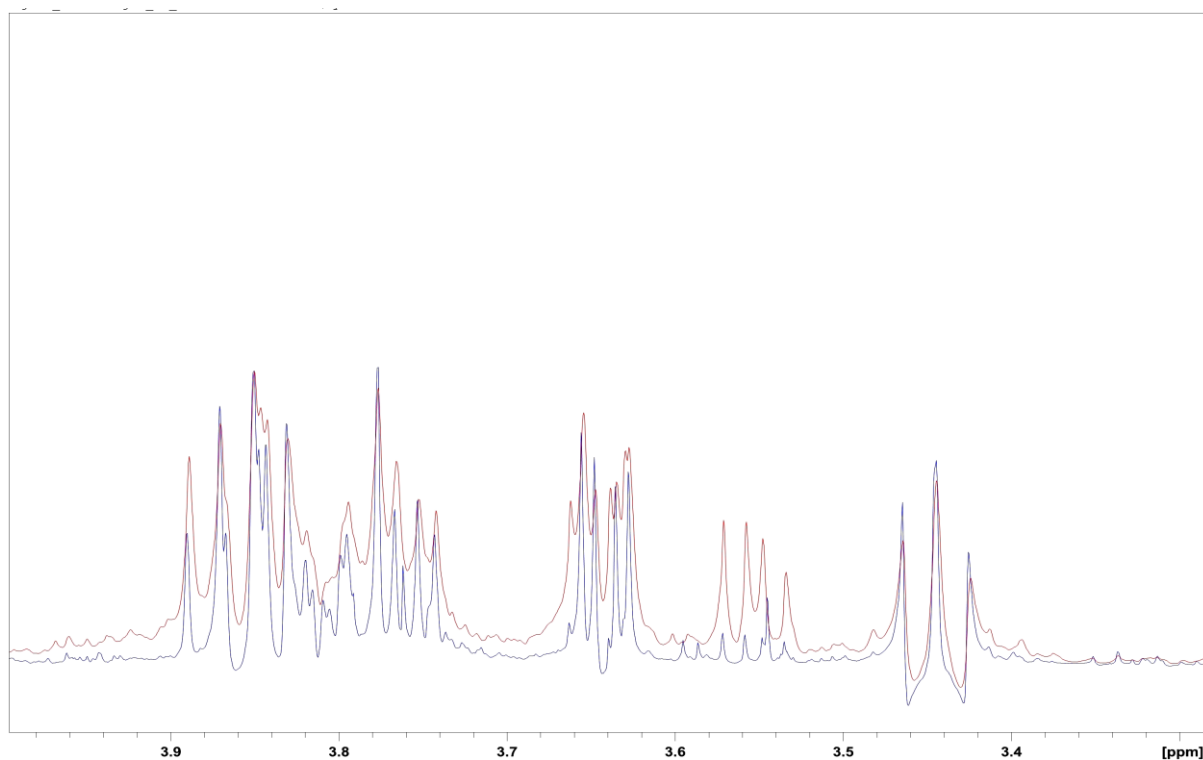

Figure 4.1.3: Yeast cell extraction spectrum from 4.0-3.3 ppm of extracts that where washed 4 (blue) and 1 (red) times respectively, according to the procedure described in 3.1 and 3.2. The extract that was washed one time shows broader and less clearly defined peaks.

Figure 4.1.3 shows the necessity of the washing procedure. The metabolites having clearly defined peaks is essential to measuring their diffusion. It is especially important because the yeast suspensions are complex samples with many of different molecules contributing to the signal.

4.2 Water suppressed spectrum of yeast suspensions.

After having identified the metabolites in the extract spectrum, that spectrum must be compared to the yeast suspension spectrum. This is not only to correlate the signals in the spectrums, but also to identify which signals are separated enough from the others to be measured in the diffusion experiment without interference from other signals.
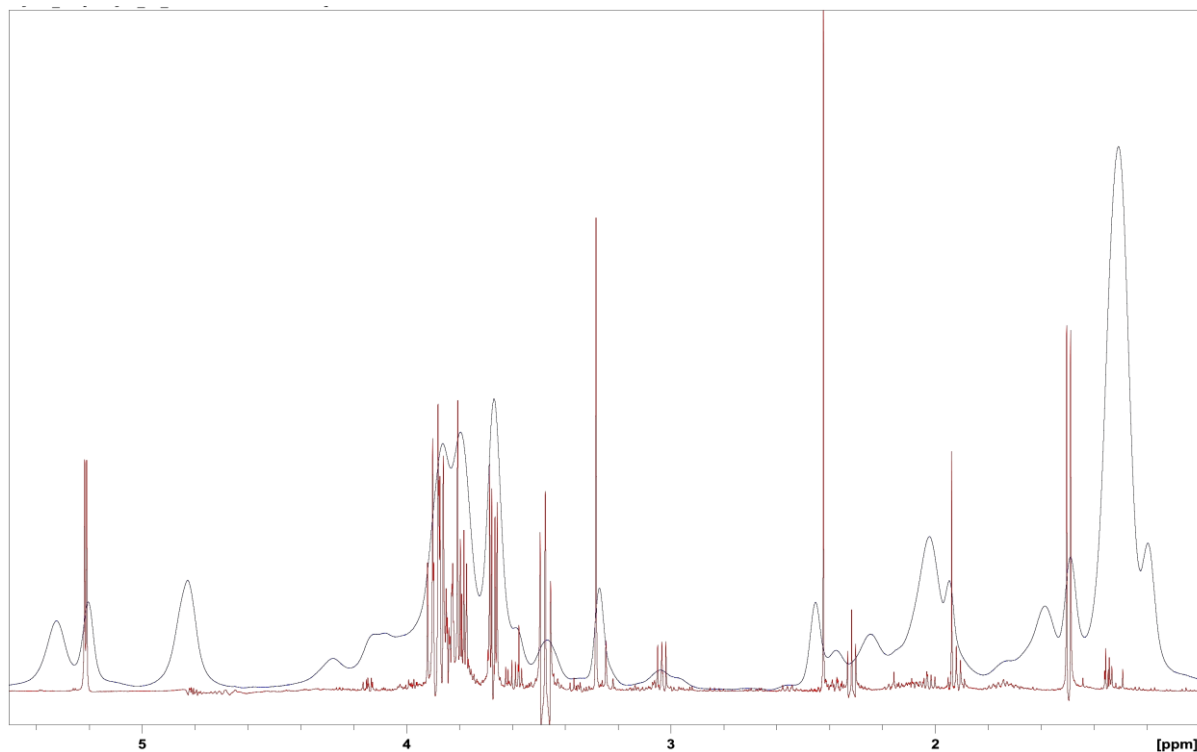
Figure 4.2.1: Water suppressed yeast suspension spectrum (blue) as compared to the extract from 4.1 (red) in the 5,5-1 ppm range.

Figure 4.2.1 shows both overlapping peaks and peaks in the suspension that do not appear in the extract. The suspension peaks are a lot broader and more overlapping with each other than the extraction peaks.
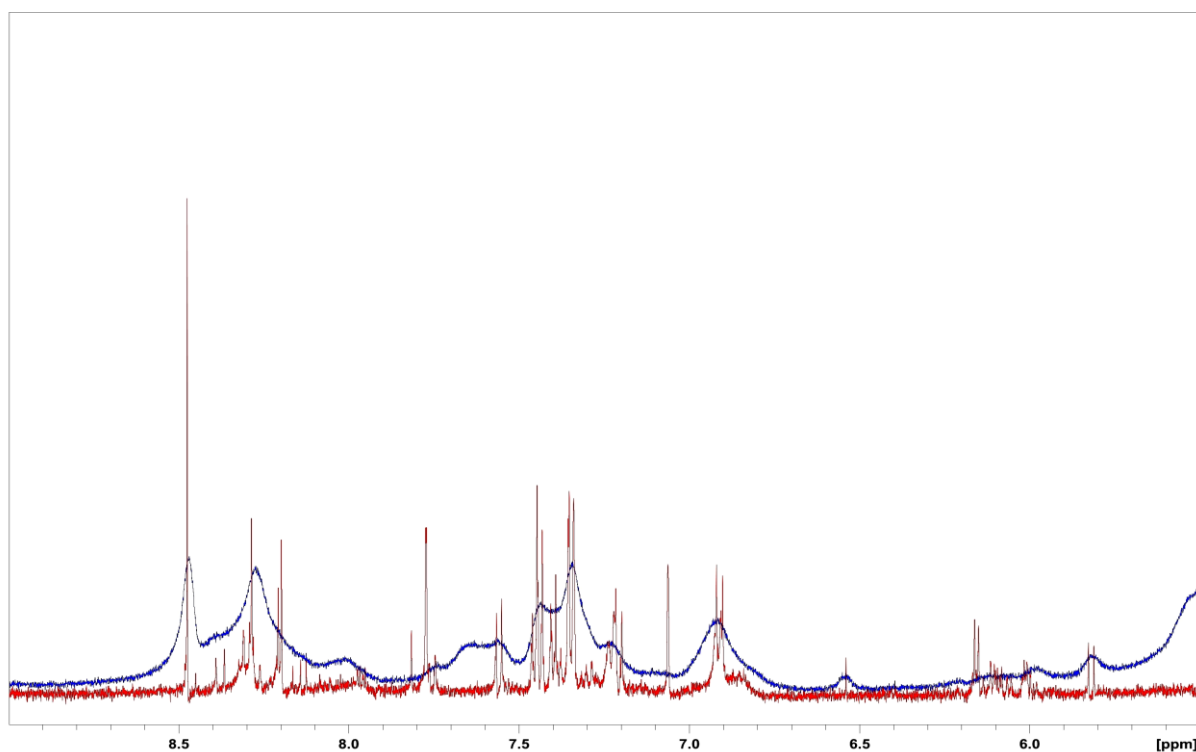
Figure 4.2.2: Water suppressed yeast suspension spectrum (blue) as compared to the extract from 4.1 (red) in the 8,5-5,5 ppm range.

Fiigure 4.2.2 shows both overlapping peaks and peaks in the suspension that do not appear in the extract. The signal to noise ratio is worse in this range, and no signals from this range were used in the diffusion experiments.
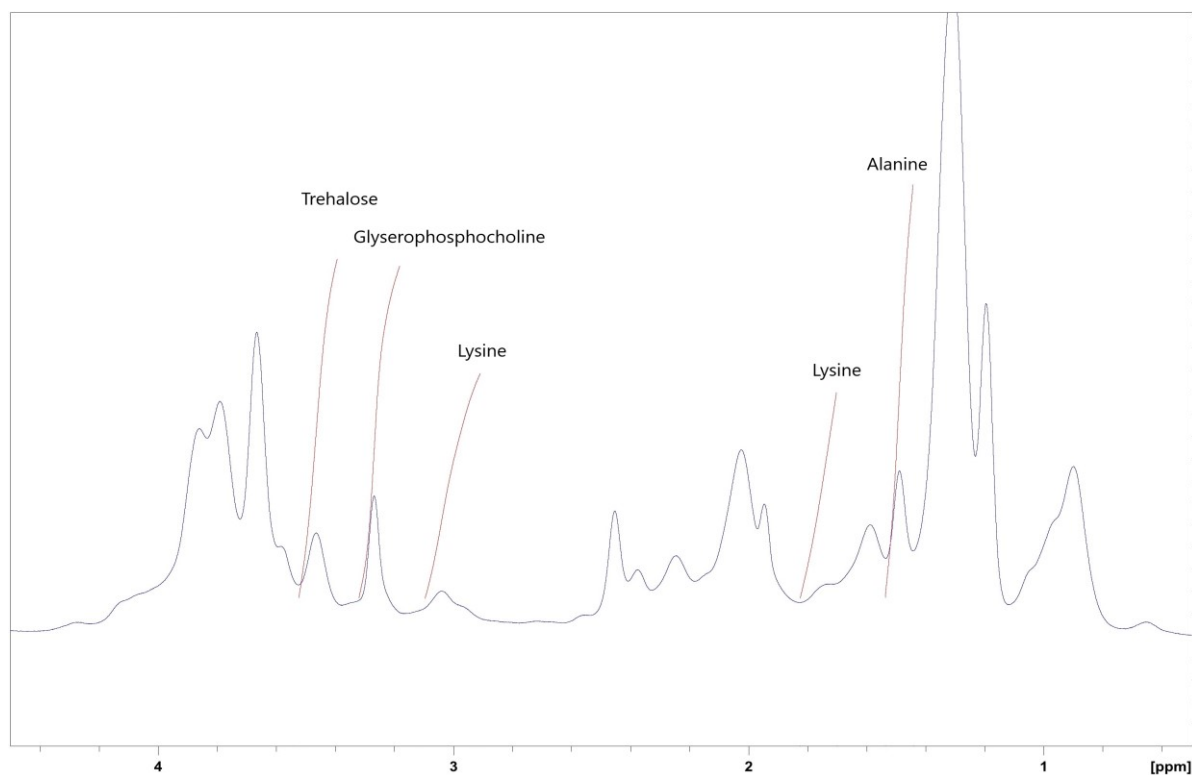
Figure 4.2.3: NMR-spectrum showing the signals that have been used in the diffusion experiments.

The signals in the figure above were selected because they were at least somewhat separable from other signals, and were seemingly made from a single metabolite. Many of the strong signals seem to contain contributions of several metabolites, and so could not be used because the metabolites would have different diffusion from each other, though the restricting effect of the environment on them should be relatively the same.
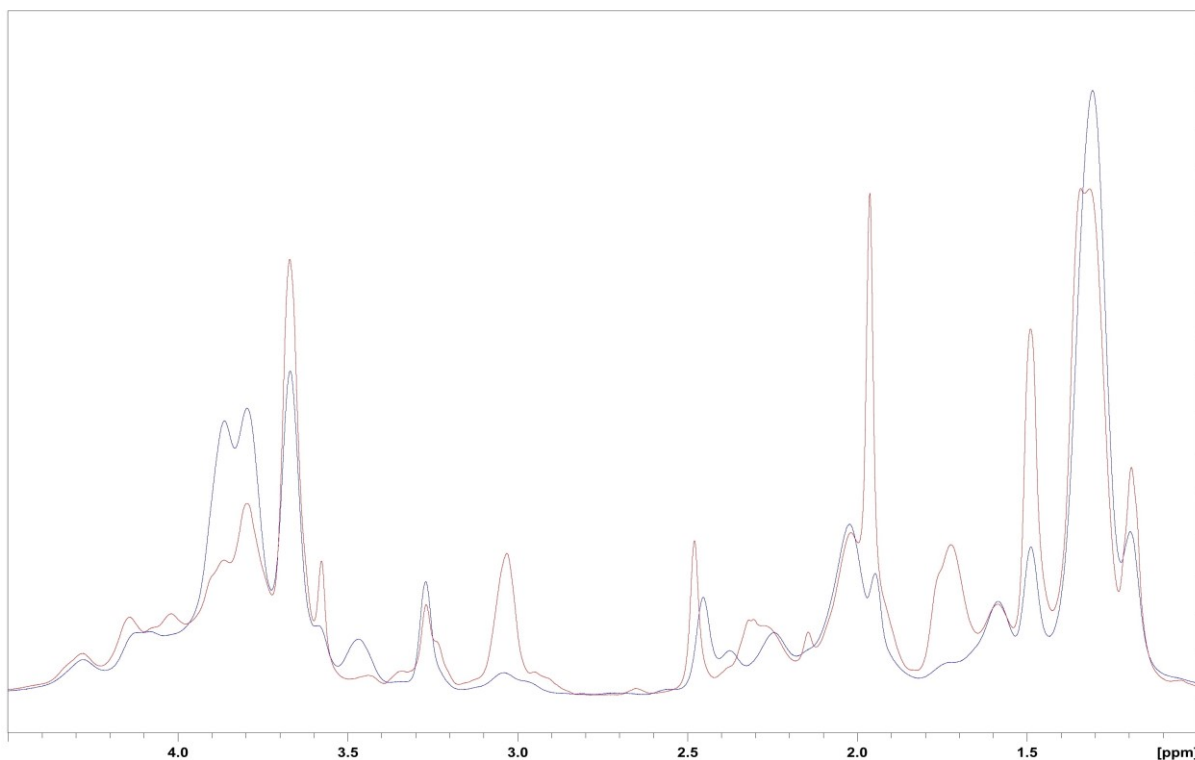
Figure 4.2.4 Shows a comparison between the spectrums of the older and the newer samples. This is specifically a water suppressed spectrum of sample 3 (blue) and of sample 4 (red), which are the same sample measured after 4 and 11 days respectively. The other two samples measured for metabolites show the same changes dependent on days suspended.

Results will show later that there is difference in measured cell size based on the suspensions age (how many days they were suspended before they were measured). Because of this it becomes interesting how the suspension spectrums change from the new to the old samples. There are several differences in the above comparison, which makes it clear that changes do occur in the cells over time. These changes could occur as a result of the cells dying and structurally breaking down.

The most relevant changes are those that occur in the measured metabolites. The Lysine signals at 3 and 1,7 ppm are both clearly more intense in the older samples, and for the one at 1,7 ppm that means there is less overlap with neighboring signals. The Alanaine signal at 1,47 ppm is also stronger in the older samples, though the change is less dramatic. Trehalose shows the opposite trend, it has a weaker signal in the older samples. Finally, the Glyserophosphocholine signal shows little change. When the signals are more intense, that should mean larger signal to noise ratio, which could mean less uncertainty in the results.

Several of the signals selected do show some overlap with different signals. Trehalose has some overlap on the left side, and the Lysine signal at 1,7 ppm has a lot of overlap on the right side. The Alanine signal is quite strong, but does have overlap on both sides. The Lysine signal at 3 ppm seems

to overlap with a signal on its right side, though it is hard to be certain of this, as the potential other signal is somewhat small. The Glyserophosphocholine signal seems to be relatively alone.

4.3 Testing a metabolite for an EC component

If the metabolites have an EC component, that could affect the measurements as the EC metabolites would not experience the same restrictions as the IC metabolites. To test this the diffusion of a yeast suspension was measured 28 times over about 20 hours with constant diffusion time. The suspension was filled higher in the NMR tube than normal. This would let the suspension sink in the tube during measurement, while the water would rise to the top, increasing the concentration of yeast cells in the sampled area. The change in yeast cell concentration is illustrated in the pictures below, though the pictures are of a different sample than the one that was measured.
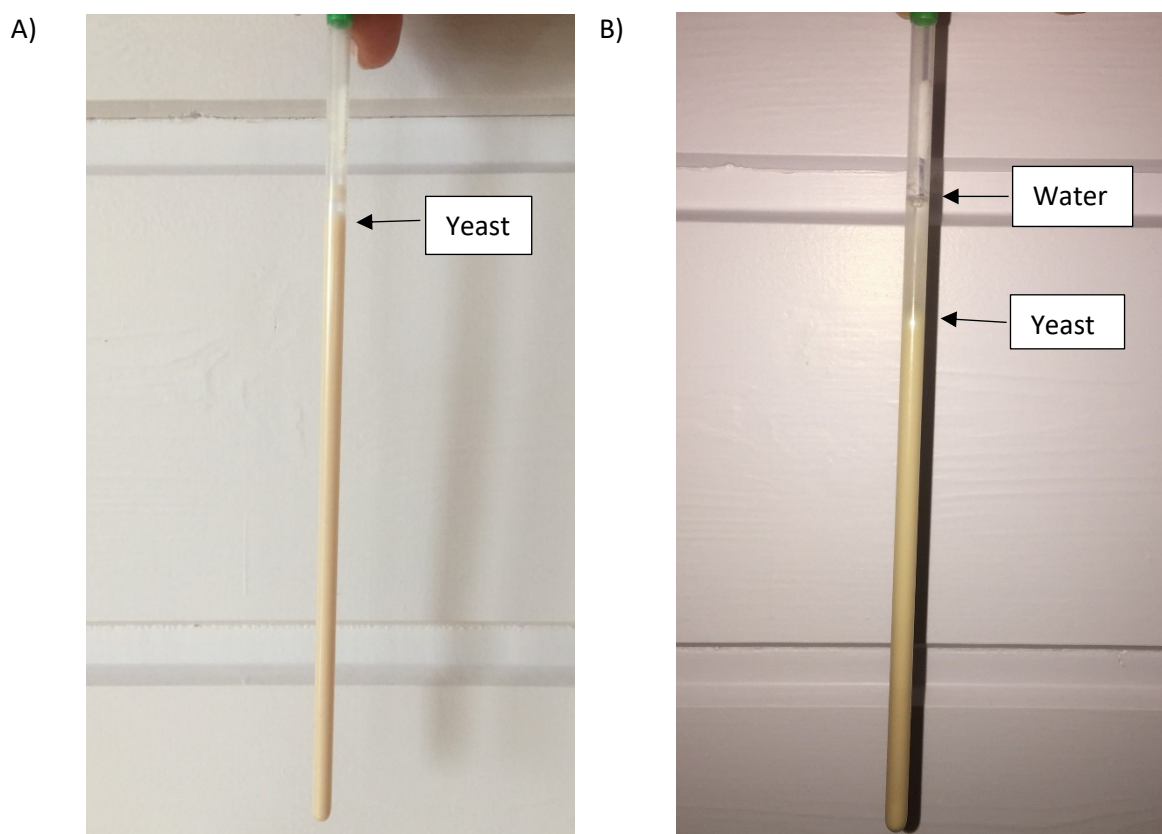
Figure 4.3.1 Yeast cell suspension sample before, A), and after, B), 20 hours. The figure does not show the sample that was actually measured on, but a similar amount of yeast would have sunk to the bottom.

Then the $\ln(M/M_0)$ vs k^2 plots from one metabolite in those measurements where fitted to a two-component solution. The ratio of intensities of those components were plotted against time below.
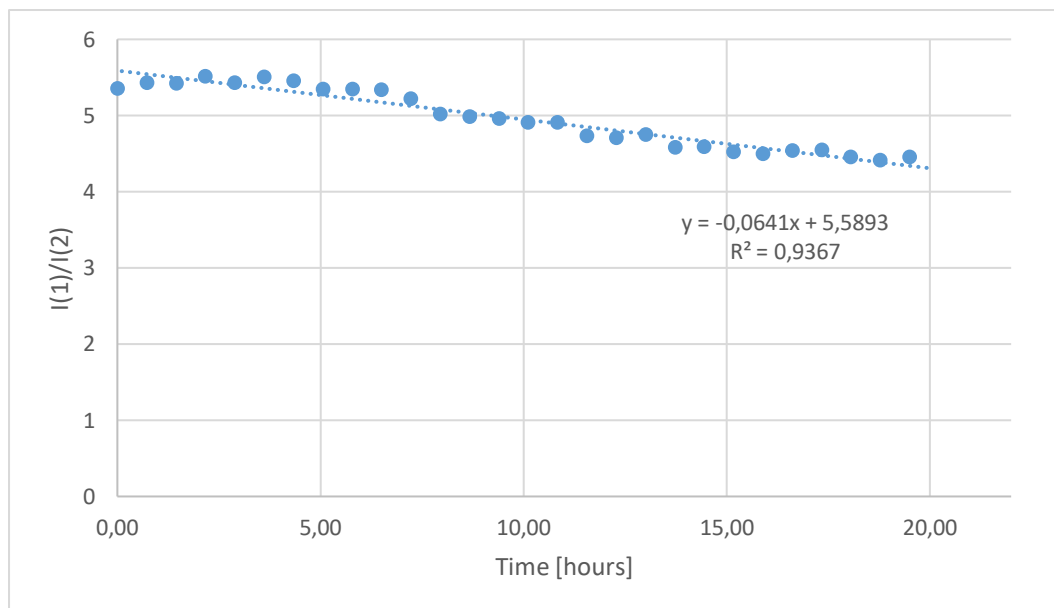
Figure 4.3.1: The ratio of the intensities of two components from $\ln(M/M_0)$ vs. k plots of Glyserophophocholine, plotted against time since start of measurements. Each experiments took 43 min and 20 s, and were run in immediate succession of each other. The first intensity, I(1), corresponds to the higher diffusion coefficient while the second corresponds to the slower.

The plot in figure 4.3.1 shows a small negative trend of -0,064±0,003. There should be a negative trend if the metabolite signal had an EC component, as the intensity of the faster EC component of the diffusion signal would lessen and the intensity of the slower IC component of the diffusion signal would increase. The negative trend is however too small in comparison to the amount of displeased water in the sample, see figure 4.3.1. This means that the metabolite having an EC component is unlikely.

The diffusion of the two components also do not seem to correspond to an EC and an IC diffusion. The first component had an average diffusion of $3,84*10^{-10}$ while the second component had and average diffusion of $8,45*10^{-12}$. As one can see in table 4.6.1, the first component is of the right order of magnitude for the IC diffusion of Glyserophosphocholine, while the diffusion of the second component is too small. Therefore, the second component is likely not an IC component, but the effect of restricted diffusion at high values of k.

4.4 Cell size measurements from metabolite diffusion

The next step to determining the cell size is plotting measured diffusion against the square root of diffusion time, as discussed in section 2.6. This was done for each sample and for each metabolite selected in section 4.2. Below follow examples of such plots for each metabolite, one as an example of the newer samples (sample 3) and one as an example the older samples (sample 4). The trends in cell size and initial diffusion will be discussed in section 4.6. The trends in uncertainty between new and old samples, if any, are discussed here.
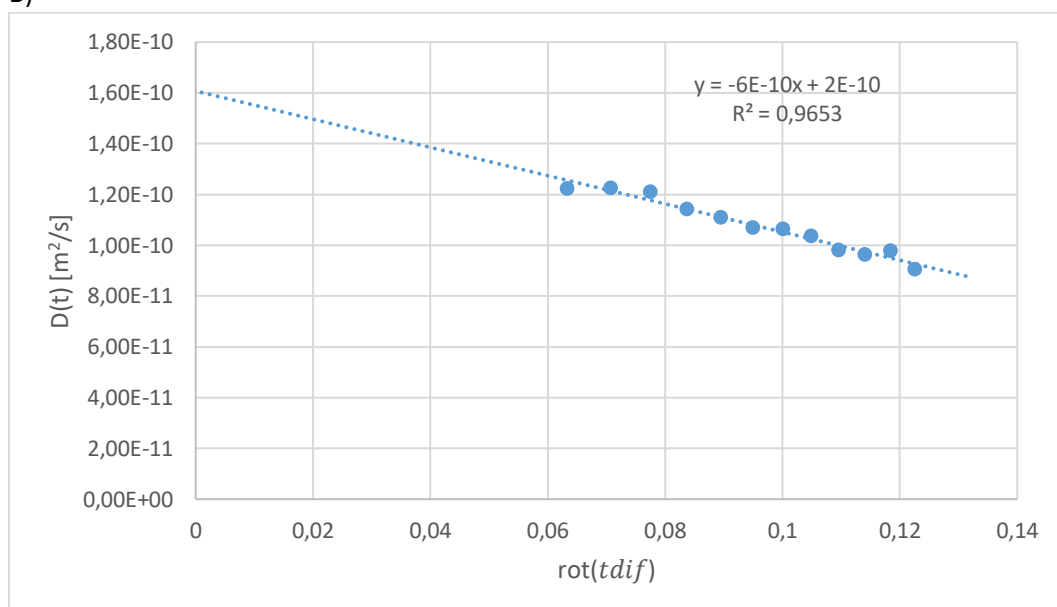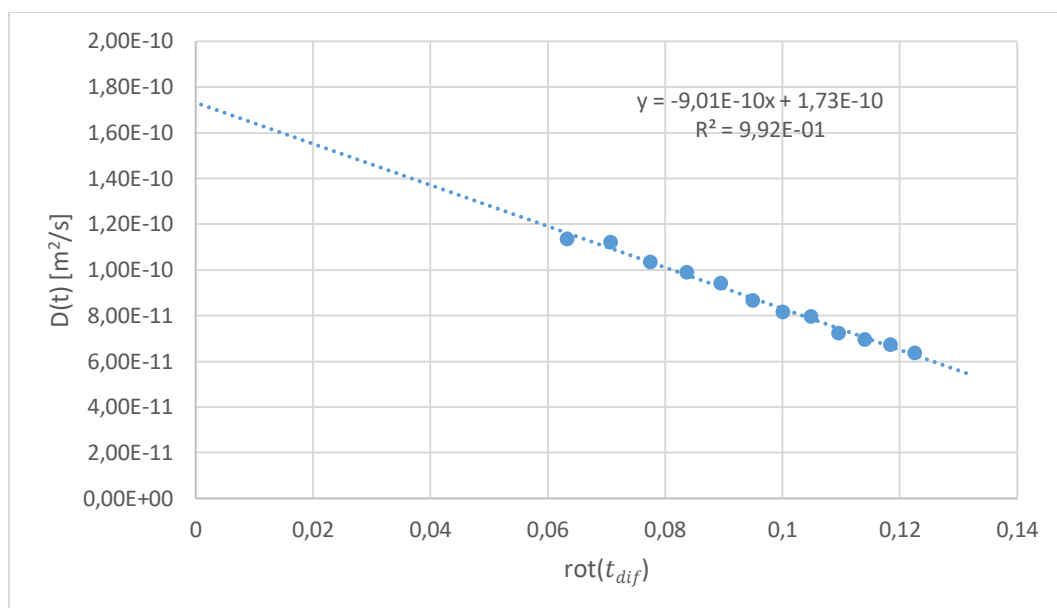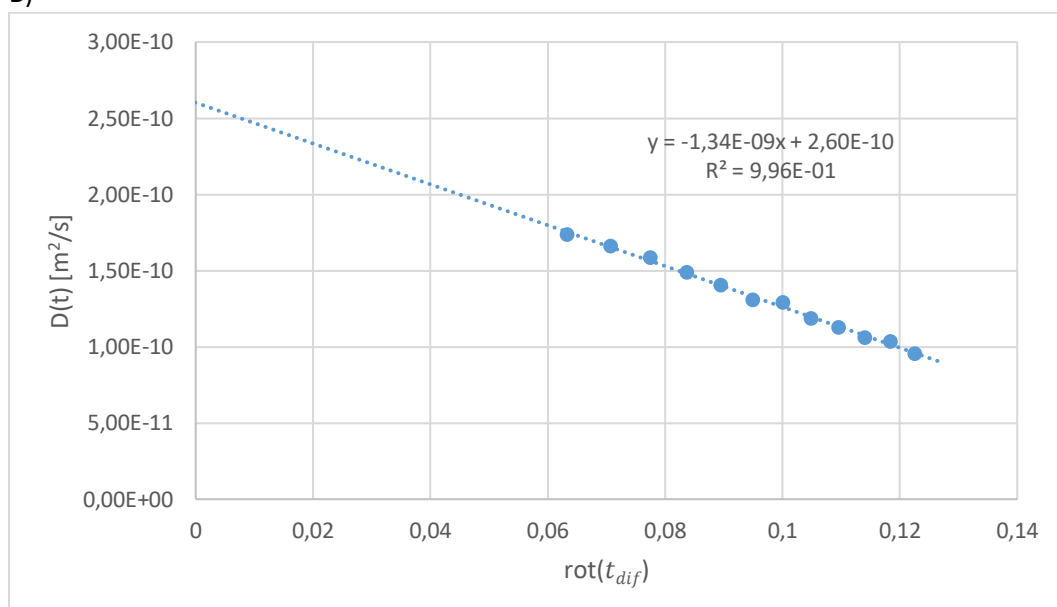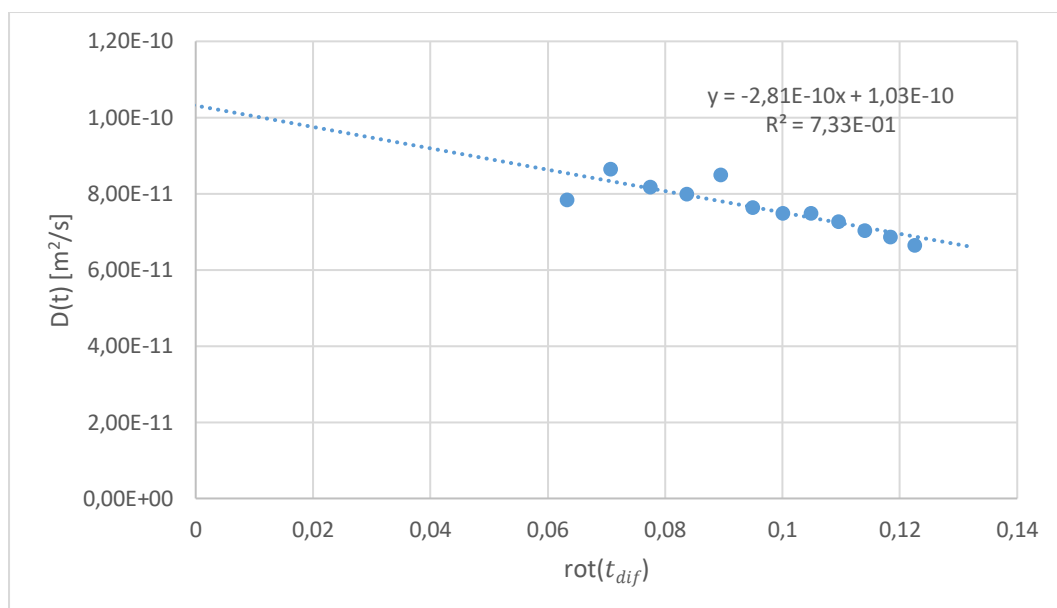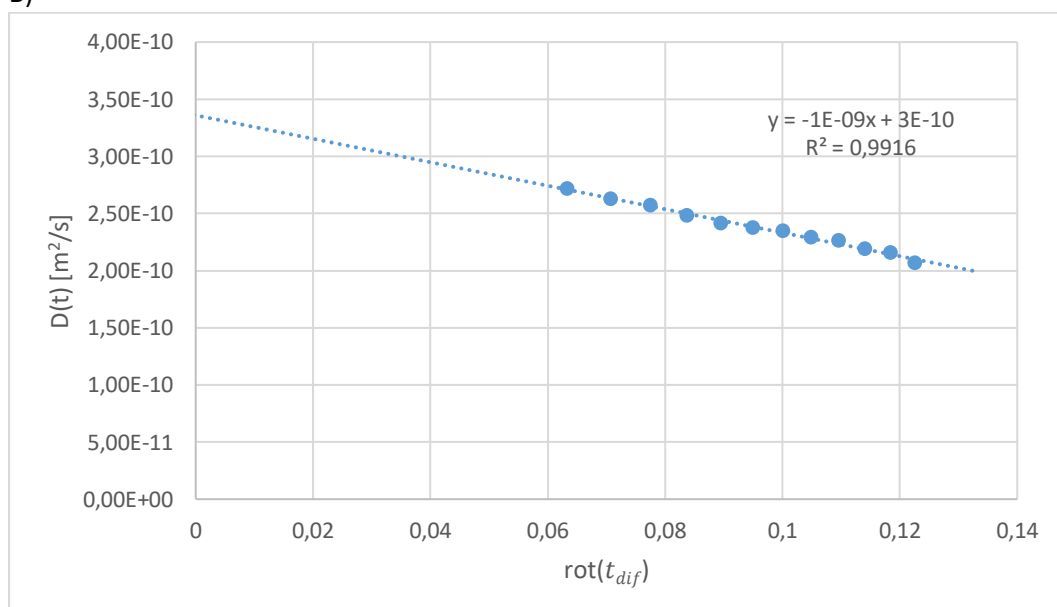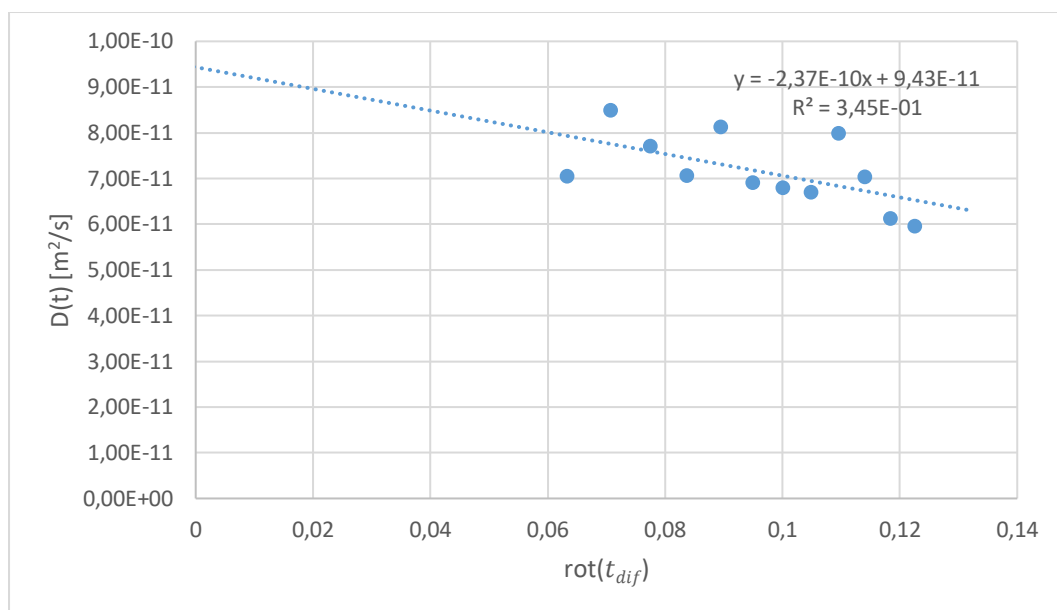
A)
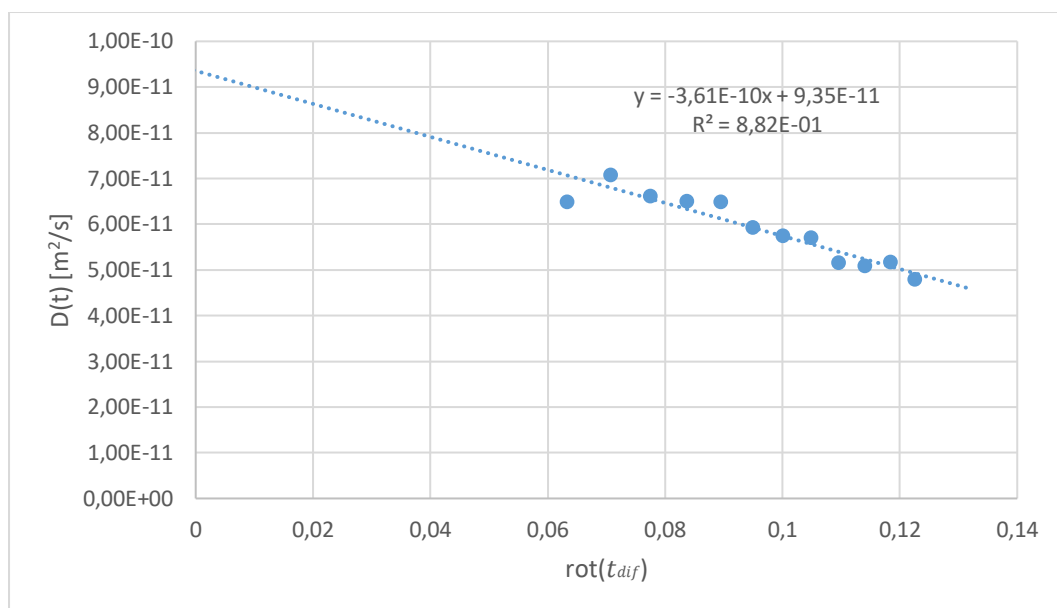
B)

Figure 4.4.1: D(t) plotted against $\sqrt{t_{dif}}$ for the Trehalose signal at 3,4 ppm in the diffusion measurements of A) sample 3 and B) sample 4. Using equation 2.5.2 and 2.5.3 gives a cell radius of $1,9*10^{-6}$ $\pm2*10^{-7}$ m and $2,76*10^{-6}$ $\pm2*10^{-7}$ m respectively. The extrapolation back to rot(t_{dif})= 0 gave an initial diffusion coefficient of $9,3*10^{-11}$ $\pm4*10^{-12}$ m²/s and $1,60*10^{-10}$ $\pm3*10^{-12}$ m²/s respectively.

There seems to be little to no change in uncertainty for the above measurements, despite there being a stronger signal in the older yeast suspensions than the newer, as shown in figure 4.2.4. The points do seem a little more scattered in A), but the difference is not significant.

A)

B)

Figure 4.4.2: D(t) plotted against $\sqrt{t_{dif}}$ for the Glycerophosphocholine signal at 3,2 ppm in the diffusion measurements of A) sample 3 and B) sample 4. Using equation 2.5.2 and 2.5.3 gives a cell radius of $1,90*10^{-6}$ $\pm5*10^{-8}$m and $2,35*10^{-6}$ $\pm5*10^{-8}$ m respectively. The extrapolation back to rot(t_{dif})= 0 gave an initial diffusion coefficient of $1,73*10^{-10}$ $\pm3*10^{-12}$ m²/s and $2,60*10^{-10}$ $\pm3*10^{-12}$ m²/s respectively.

There is not a significant difference in the uncertainty in the measurements from figure 4.4.2. In this case that was expected, as there is no discernible change in signal in figure 4.2.4.

A)

B)

Figure 4.4.3: D(t) plotted against $\sqrt{t_{dif}}$ for the Lysine signal at 3,0 ppm in the diffusion measurements of A) sample 3 and B) sample 4. Using equation 2.5.2 and 2.5.3 gives a cell radius of $2,8*10^{-6} \pm 5*10^{-7}$ and $4,51*10^{-6} \pm 1*10^{-7}$ m respectively. The extrapolation back to rot(t_{dif})= 0 gave an initial diffusion coefficient of $1,03*10^{-10} \pm 5*10^{-12}$ m^2/s and $3,35*10^{-10} \pm 3*10^{-12}$ m^2/s respectively.

The measurements in figure 4.4.3 have a big change in the uncertainty of the cell radius from A) to B). That would point towards the increased signal in figure 4.2.4 having an effect. However, the other new sample, sample 1, did not have the large uncertainty that sample 3 has here (see table 4.6.1 for specific numbers). This points towards sample 3 simply being somewhat of an outlier, as opposed to the uncertainty being the results of a trend. What caused this is hard to say, but something in the cell likely interfered with the Lysine signal.
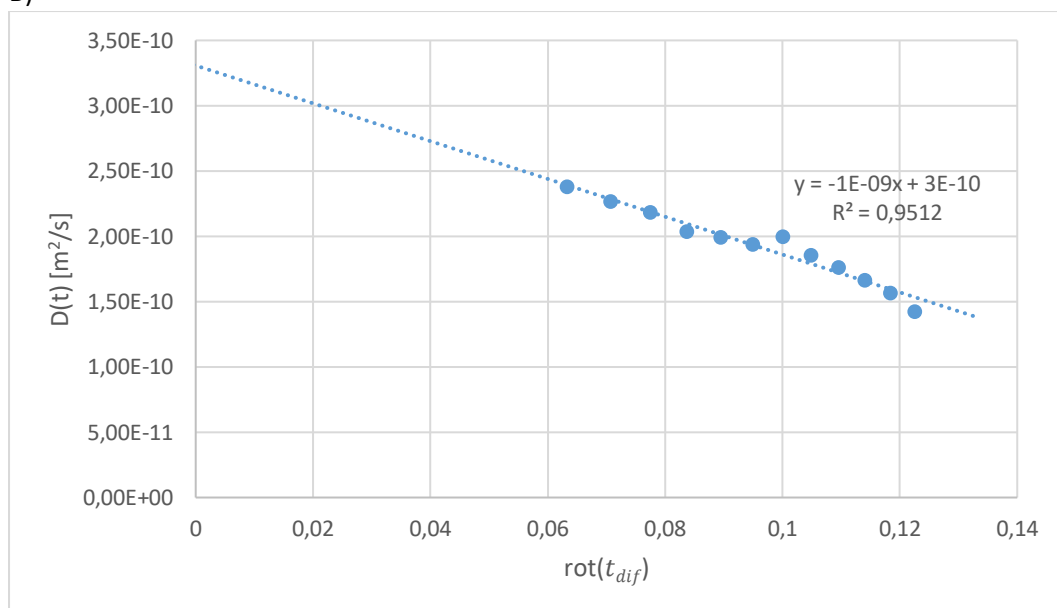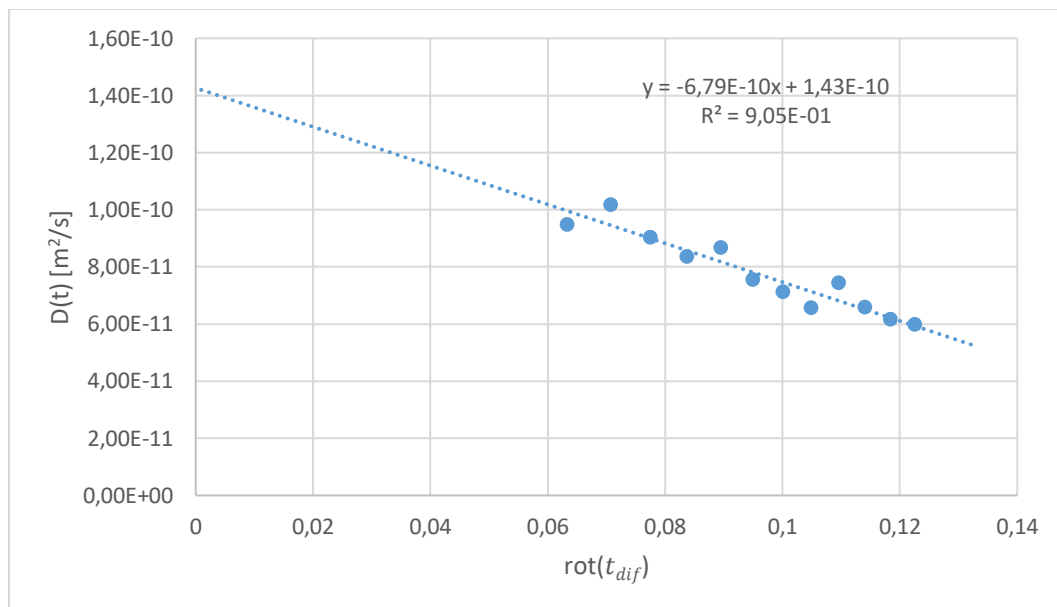
A)

B)

Figure 4.4.4: D(t) plotted against $\sqrt{t_{dif}}$ for the Lysine signal at 1,7 ppm in the diffusion measurements of A) sample 3 and B) sample 4. Using equation 2.5.2 and 2.5.3 gives a cell radius of $3*10^{-6} \pm 1*10^{-6}$ m and $2,8*10^{-6} \pm 2*10^{-7}$ m respectively. The extrapolation back to $rot(t_{dif})= 0$ gave an initial diffusion coefficient of $9,4*10^{-11} \pm 1*10^{-11}$ m²/s and $3,3*10^{-10} \pm 1*10^{-11}$ m²/s respectively.

The second Lysine signal, shown in figure 4.4.4, has a similar, even larger change in uncertainty as the one from figure 4.4.3. It is also similar in that the other new sample, sample 1, had an uncertainty that was closer to the older samples. It is likely that whatever caused the Lysine signal to be an outlier in figure 4.4.3 A), also caused it to be an outlier here. The signal from the new yeast does overlap a lot with a neighbouring signal in figure 4.2.4, and that may have contributed to the uncertainty being this large.
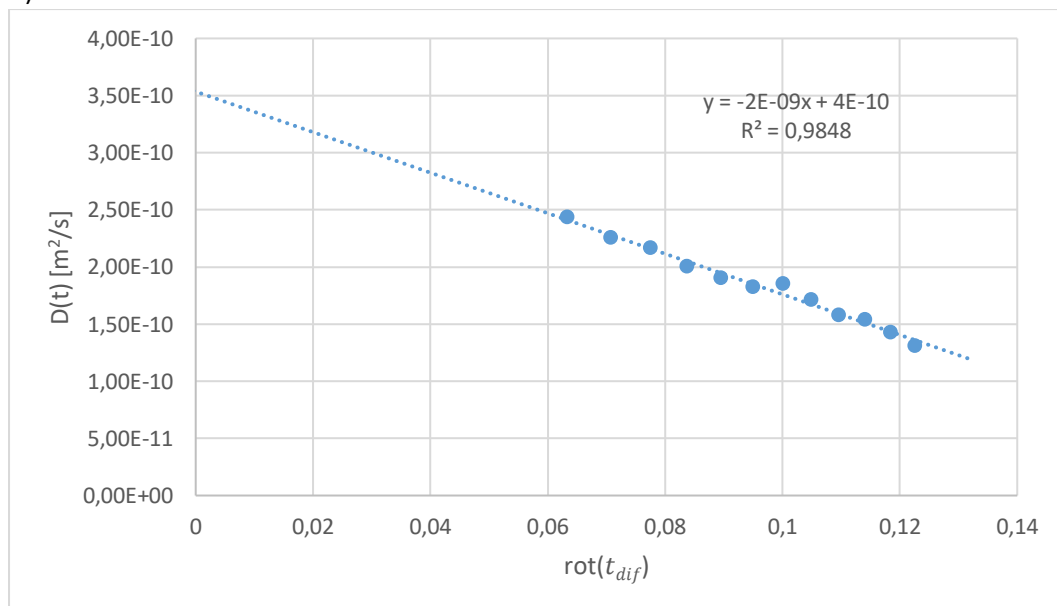
A)

B)

Figure 4.4.6: D(t) plotted against $\sqrt{t_{dif}}$ for the Alanine signal at 1,5 ppm in the diffusion measurements of A) sample 3 and B) sample 4.The Using equation 2.5.2 and 2.5.3 gives a cell radius of $1,9*10^{-6} \pm 2*10^{-7}$ m and $2,82*10^{-6} \pm 1*10^{-7}$ m respectively. The extrapolation back to rot(t_{dif})= 0 gave an initial diffusion coefficient of $1,42*10^{-10} \pm 7*10^{-12}$ m^2/s and $3,53*10^{-10} \pm 7*10^{-12}$ m^2/s respectively.

There also is not much change in uncertainty in the measurements in figure 4.4.6. The Alanine had a small increase in signal from new to old yeast, but this does not seem to have had much effect.

Overall, there seems to be little correlation between the changes in signal illustrated in figure 4.2.4 and the uncertainties. Therefore, that level of signal to noise ratio change is probably not large enough to have a significant effect on the uncertainties. There are likely other factors that have an effect, such as other signals in the yeast cell suspension that interfere with the metabolite signal.

Glyserophosphocholine does seem to have slightly smaller uncertainties that the other metabolites. Glyserophosphocholine is probably in an area of the spectrum with less interference from other signals. There is no observed overlap with other signals for Glyserophosphocholine in figure 4.2.4.

4.5 Cell size measurements from intracellular water

Below is the same measurements as for the previous section, but for the IC water signal. Again, changes in cell size and initial diffusion will be discussed in section 4.6.
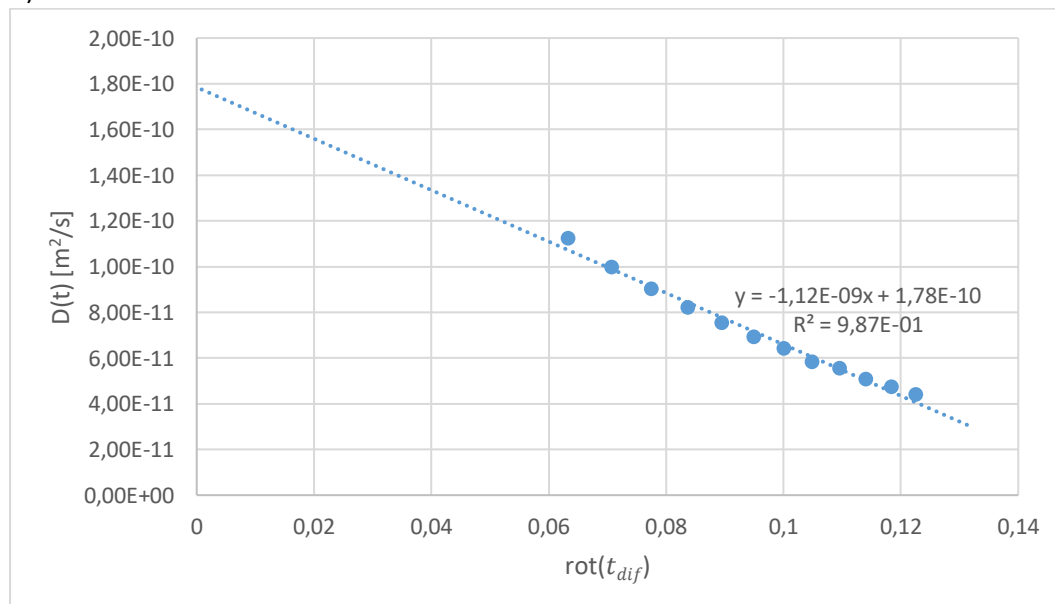
A)
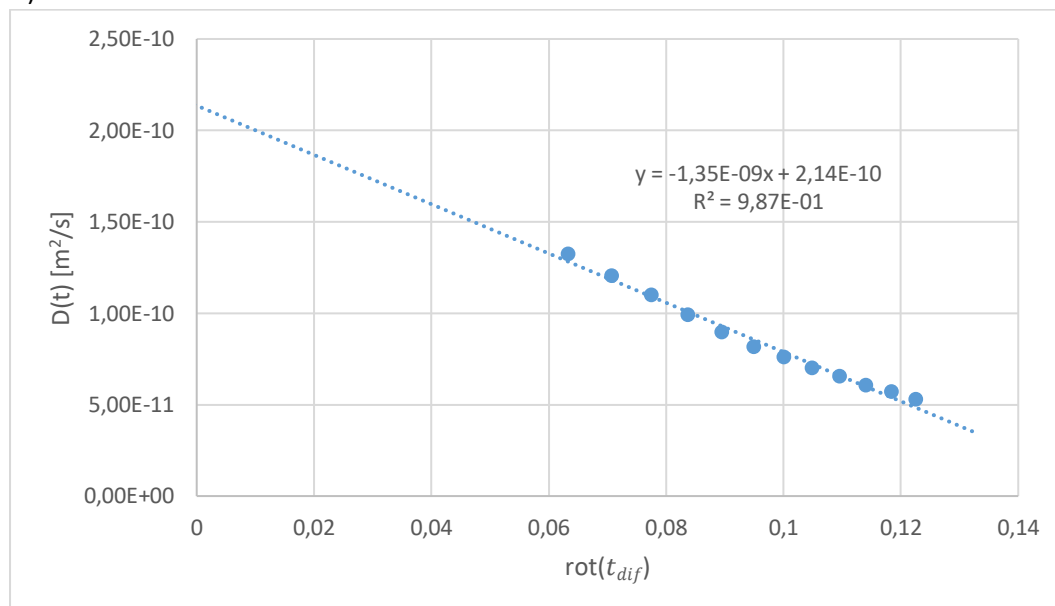
B)

Figure 4.5.1: D(t) plotted against $\sqrt{t_{dif}}$ for the intracellular component of the water in the diffusion measurements of A) sample 3 and B) sample 4. Using equation 2.5.2 and 2.5.3 gives a cell radius of $1{,}74*10^{-6}$ $\pm6*10^{-8}$ m and $1{,}59*10^{-6}$ $\pm4*10^{-8}$ m respectively. The extrapolation back to rot(t_{dif})= 0 gave a initial diffusion of $2{,}13*10^{-10}$ $\pm5*10^{-12}$ m²/s and $1{,}78*10^{-10}$ $\pm4*10^{-12}$ m²/s respectively.

There is also no large change in the uncertainty of the measurements from the IC water signal in figure 4.5.1. These measurements do have smaller uncertainties than the metabolites in general, in the range of Glyserophosphocholine, despite using the whole of the $\ln(M/M_0)$ vs k . curve. This makes sense, as there is a lot more water signal, so the signal to noise ratio would be larger for water than the metabolites.

4.6 Cell radius measurements over time

It was mentioned before that there are some changes in cell size from older to newer cells. That will be examined further in this section. Below is a table showing all the measured cell radii and extrapolated initial diffusions.

Table 4.6.1: Table showing all measured cell radii [m] and extrapolated unrestricted diffusions [m^2/s], as well as each metabolites molecular weight. The # column shows how many days the sample was suspended.

	#		IC Water	Trehalose	Glyceropho-sphocholine	Lysine 3,0 ppm	Lysine 1,7 ppm	Alanine
M_w	-	-	18,01	342,30	257,22	146,19	146,19	89,09
1	3	R	-	1,7±0,2E-06	1,80±0,07E-06	2,0±0,1E-06	2,1±0,3E-06	1,9±0,1E-06
		D_0	-	9,4±0,4E-11	1,86±0,04E-10	1,68±0,07E-10	1,8±0,1E-10	2,03±0,09E-10
2	5	R	1,69±0,05E-06	-	-	-	-	-
		D_0	1,97±0,03E-10	-	-	-	-	-
3	4	R	1,74±0,06E-06	1,9±0,2E-06	1,90±0,06E-06	2,8±0,5E-06	3±1E-06	1,9±0,2E-06
		D_0	2,14±0,05E-10	9,4±0,4E-11	1,73±0,03E-10	1,03±0,05E-10	9±1E-11	1,43±0,07E-10
4	11	R	1,59±0,04E-06	2,8±0,2E-06	2,36±0,05E-06	4,5±0,1E-06	3,1±0,2E-06	2,8±0,1E-06
		D_0	1,78±0,04E-10	1,61±0,03E-10	2,60±0,03E-10	3,36±0,03E-10	3,3±0,1E-10	3,53±0,07E-10
5	12	R	1,34±0,07E-06	3,7±0,3E-06	2,81±0,09E-06	4,9±0,3E-06	3,2±0,2E-06	3,3±0,2E-06
		D_0	1,22±0,04E-10	1,74±0,04E-10	2,56±0,03E-10	2,87±0,05E-10	2,68±0,06E-10	3,2±0,1E-10

These cell radii are of a reasonable magnitude for yeast. In their study of stratification of yeast cells, Svenkrtova et.al. [33] separated their cells into categories with mean cell radius ranging from $1,9*10^{-6}$ m to $3,3*10^{-6}$ m. The newer cells here would be on the smaller size in that study, and the older cells would be on the larger side, but both completely within what is reasonable.

It is hard to know how exact the model is, since yeast is somewhat variable in size depending on strain and growing time. One can see that this method of measuring cell size gives reasonably consistent numbers within each sample, but to determine the presence of any systematic errors one would have to verify the cell size of the same samples with a different method.

Below is a figure showing trends in cell radius. Since there are only effectively four measured samples, any trends are not very strongly supported. This is especially true for the water signal, as it does not have five measurements for each sample, which the metabolites have collectively.
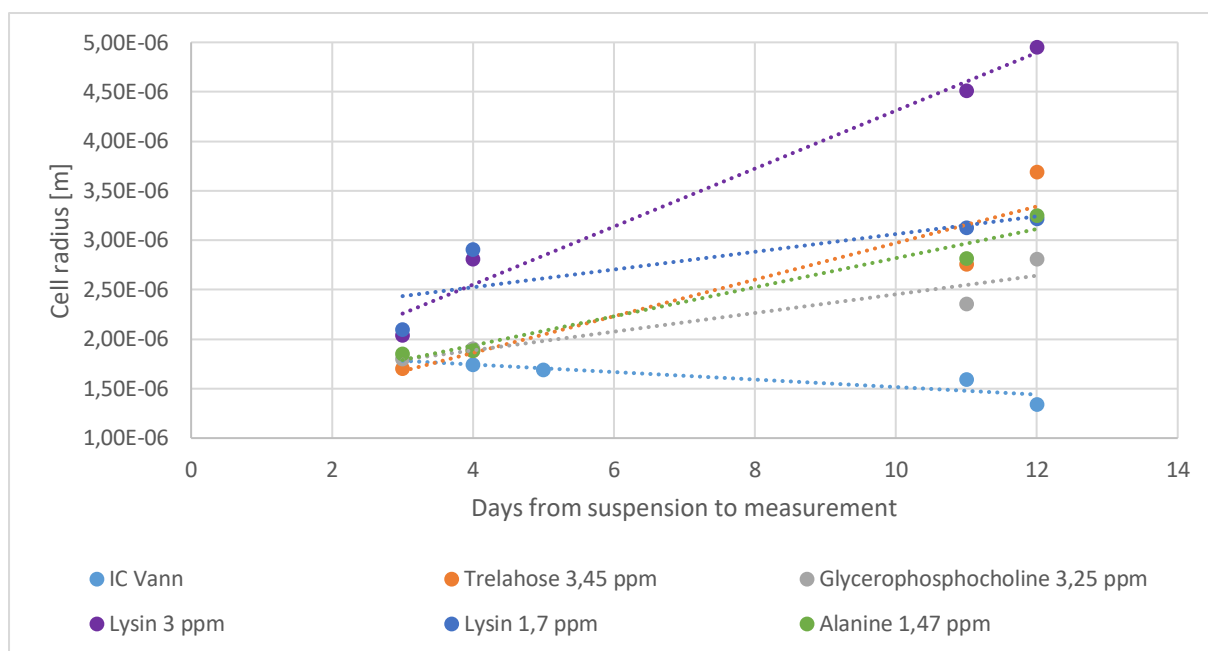
Figure 4.6.1: Calculated cell radii from different measurements plotted against how long they were suspended before measurement. All metabolites show increase in radius with increased days, with Lysine at 3,0 ppm showing strongest growth. That growth does not appear to be present in the IC water signal.

The results in figure 4.6.1 show that the apparent cell radius grows when left suspended for an extra week. As the cells are previously dried, there should be no growth in the yeast cells. A possible reason for that appearance of growth is that the plasma wall is deteriorating because some cells are dying. If this is the case the hindering of the diffusion could measure as smaller in the section 4.4 figures, which would give a larger measured cell radius. Helmer et.al. encountered a similar trend in their measurements of necrotic and non-necrotic tumor tissue [Helmer]. Another possibility is that there is some actual swelling in the cells, which would measure in the same way.

The water signal shows none of the growth in cell size present in the metabolite signals. This could be because there is also a lot of EC water signal, which could influence the IC water signal. Another possibly contributing factor is that if the cells are dying this could increase how much both the metabolites and the water is transferred over the cell membrane. However, water is already transferred over that membrane a lot, so the difference would be much smaller for the water than for the metabolites, where there should be virtually no transferring. Either way, it would mean that the water signal is less sensitive to IC microstructural changes then the metabolite signal. Despite the water measurements have less uncertainty in the measurements, they might give less accurate results.

Figure 4.6.1 shows that the cell size of the two Lysine signals are very close for the newer samples, but for the older samples the 3 ppm signal measures a much larger size than the 1,7 ppm signal. It is likely that this is caused by some interference from a neighboring signal in the spectrum.

The next figure shows the trend in initial diffusion. If the change in cell size is caused by the cells dying then there should theoretically be no change in this, since those microstructural changes should not have an effect on the diffusion when there has been no time for any restrictions to hinder the movement of the molecules. A swelling in the cell could change the IC density, which could cause an increase in initial diffusion.
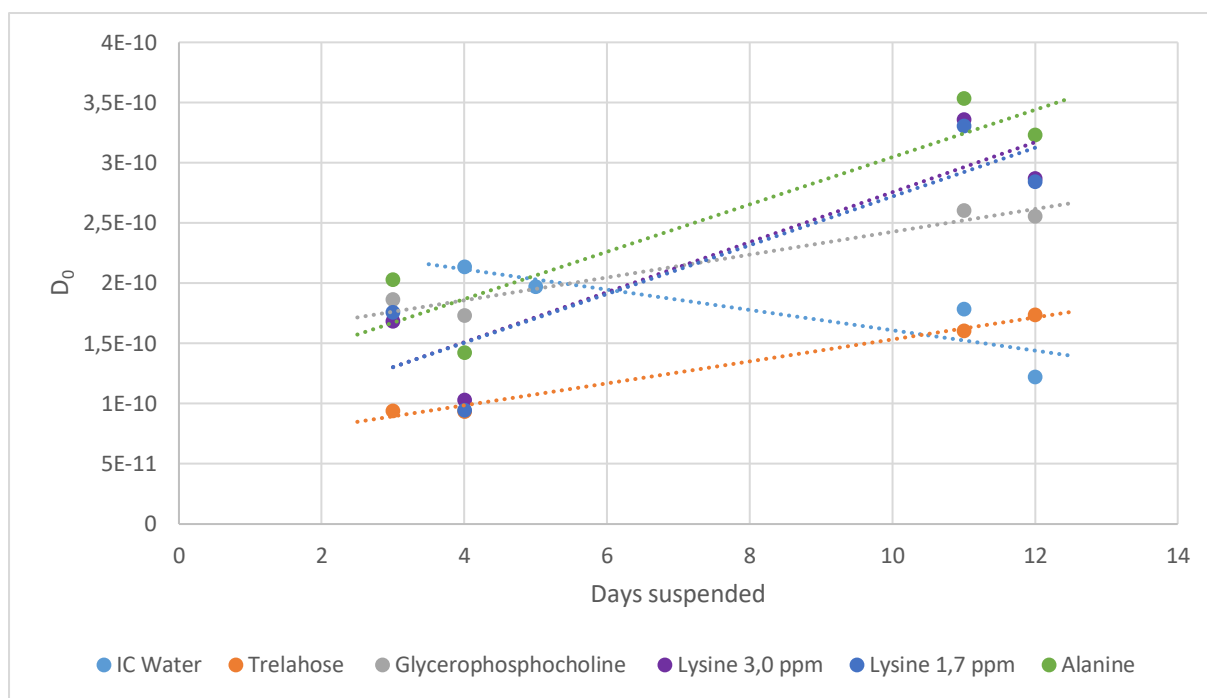
Figure 4.6.2: Extrapolated initial diffusion plotted against how many days the samples were suspended. All metabolites show increase in initial diffusion with increased days. That growth does not appear to be present in the IC water signal, instead there seems to be a decrease.

The figure above shows that the older suspensions also show an increase in initial metabolite diffusion. As mentioned above this should not be the case if the cell size growth is caused by the cells dying, as the changes in microstructure should not affect the initial diffusion. The change in initial diffusion is probably present because the extrapolations are based on the measurements from the time dependent diffusions, which are affected by changes is microstructure. The extrapolation is likely imperfect in that it is sensitive to changes in time dependent diffusion. This is also why the water signal initial diffusion shows a similar trend to the trend of the water signal cell size. If the increase in cell size is caused by swelling, then the increase in initial diffusion might be due to a lowering of IC density.

Section 2.2 says that the bigger molecules usually moves slower than the smaller ones. Therefore, the metabolites with smaller molecular weight should mostly have a higher initial diffusion. This is not always true, because the rate of movement also depends on molecular structure, but generally holds for this figure when comparing to the molecular weights in table 2.6.1. Trehalose has the highest molecular weight, and the trend line for its initial diffusion is the lowest of the metabolites. Alanine is the molecule with lowest molecular weight, and has the highest trend line for its initial diffusions. Glyserophosphocholine is heavier than Lysine, and should have ha lower initial diffusion. This is true for the older samples but the newer ones seem to have higher initial diffusions than would be expected from the molecular weights. This could be from interference from other signals on some measurements, or from molecular structure making the diffusion coefficients for Glyserophosphocholine and Lysine closer. It could also be caused by some combination of those factors.

The diffusion of the two Lysine signals are very close for each sample. This makes sense, since the signals should be coming from the same molecules, and should therefore have the same diffusion. Whatever caused the difference in cell size does not seem to have affected the measured initial diffusion.

4.7 Slice selective measurements

To examine further the diffrences between the new and old samples, slice selcetive measurements were made on samples that contained both in layers.
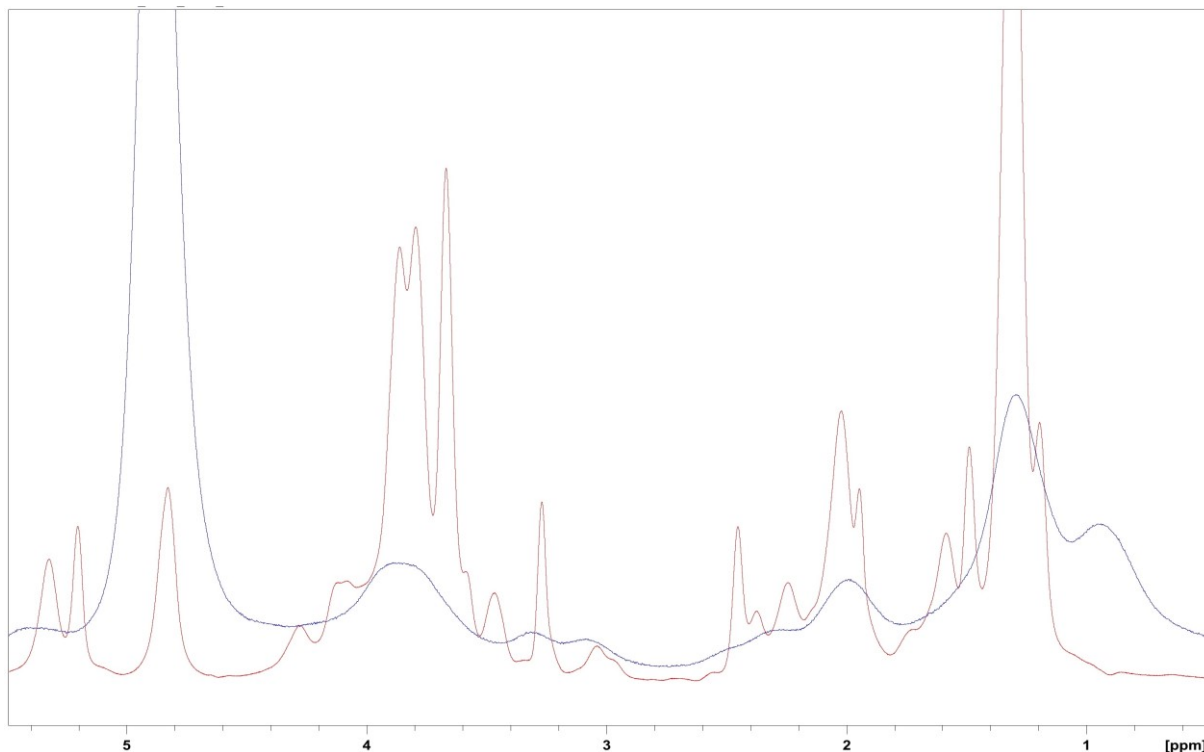

Figure 4.7.1 Comparison of spectrums of the metabolites in the slice selective measurements 3 mm below centre (blue) versus a water suppressed spectrum of a yeast suspension (red). The peaks in the slice selective measurements are much broader than those in the normal water suppressed spectrum.

The figure above shows that the measurements of the older yeast in the slice selective had very broad peaks. This is a sign of bad shimming, meaning that the magnetic field is inhomogeneous in an uncontrolled way. The bad shimming likely comes from different equipment with worse quality glass, and differing volume and geometry. The newer yeast did not have this problem with shimming, in either of the two sets of measurements.

The points in the ln(M/M_0) vs. k^2 plots conformed less to a trend for these measurements. Therefore, using only the initial k-values did not give usable results, and the curve of all the k-values was used instead. As discussed in section 2.9 this can lead to problems as the points in the ln(M/M_0) vs. k^2 plot start deviating from Gaussian behaviour for higher values of k in a restricted environment.

Because of the problems with shimming, there was a lot of overlap of signals in the spectrum, and so only the Lysine metabolite signal at 3 ppm was measured. Below follows the plots of measured diffusion against the square root of diffusion time for that signal.
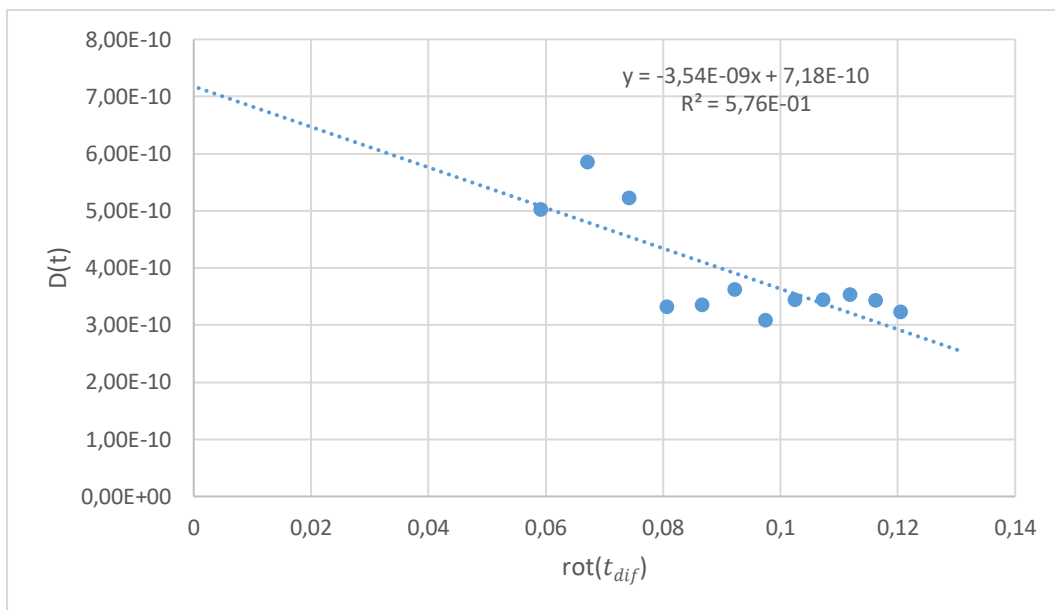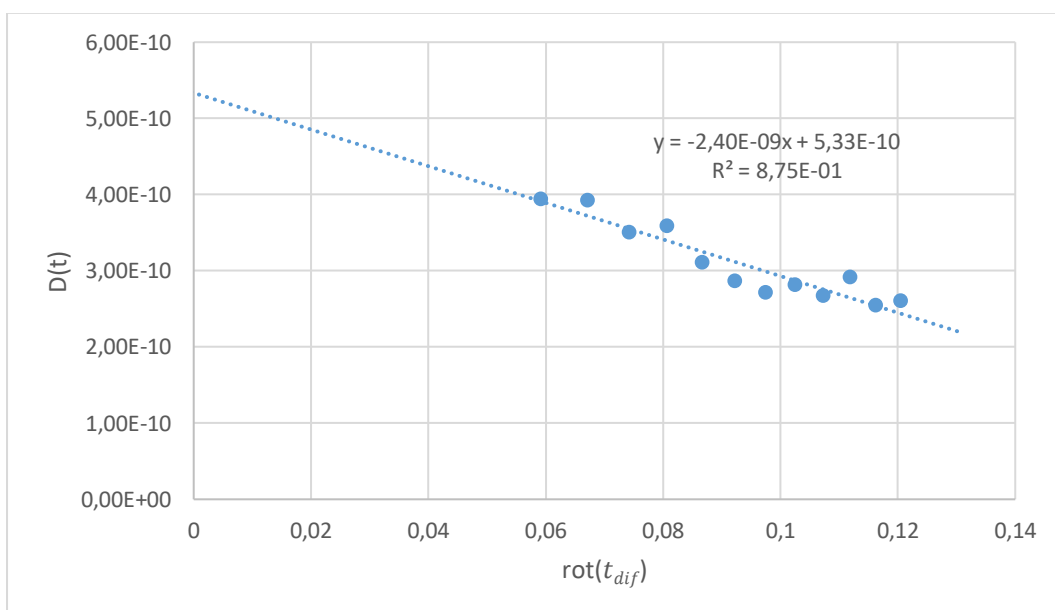
Figure 4.7.2 D(t) plotted against $\sqrt{t_{dif}}$ for the Lysine signal at 3,0 ppm in the 26.08.19 slice selective diffusion measurements of a yeast cell suspension 3 mm below center, with the 12 day old suspension. Using equation 2.5.2 and 2.5.3 gives a cell radius of $4*10^{-6}$ $\pm1*10^{-6}$ m and an initial diffusion of $7,2*10^{-10}$ $\pm9*10^{-11}$ m²/s. A repetition of the experiment gave a cell radius of $4*10^{-6}$ $\pm3*10^{-6}$ m and an initial diffusion of $5*10^{-10}$ $\pm2*10^{-10}$ m²/s.

Figure 4.7.3 D(t) plotted against $\sqrt{t_{dif}}$ for the Lysine signal at 3,0 ppm in the 26.08.19 slice selective diffusion measurements of a yeast cell suspension 3 mm above center, with the 3 day old suspension. Using equation 2.5.2 and 2.5.3 gives a cell radius of $3,9*10^{-6}$ $\pm4*10^{-7}$ m and an initial diffusion of $5,3*10^{-10}$ $\pm3*10^{-11}$ m²/s. A repetition of the experiment gave a cell radius of $3,9*10^{-6}$ $\pm9*10^{-7}$ m and an initial diffusion of $4,9*10^{-10}$ $\pm5*10^{-11}$ m²/s.

The cell sizes measured here are larger than the non-slice selective diffusion measurements. The differing equipment or geometry should not have an effect on the cell size. Neither should the use of

the full $\ln(M/M_0)$ vs. k^2 plots. The latter especially, as the water signal was measured in the same way as in the non-selective measurements, with a two component solution, and the same cell radius increase is observed for the water signal further down. The above factors could have an effect on the uncertainties, which were fairly large in the cell radii and the initial diffusion times, as compared to the non-slice selective measurements.

The larger cell sizes is hard to explain. However, it could be that since the measurements were off center, the gradient in the measured area was lower than what was calibrated for. This would cause an appearance of larger cell size.

The initial diffusion coefficients of the Lysine signal were also larger for these measurements as compared to the non-slice selective ones. They had a parallel growth to the cell sizes, in that they were all a little larger than the largest diffusion coefficients in section 4.6. The growth in apparent cell size probably affected the extrapolation to initial diffusion in the same was as it did for older and newer cells in section 4.6.

The difference between the radius measured by the metabolites of the newer and the older cells is much smaller for the slice selective measurements. In fact, for the slice selective measurements the difference in radii are within the uncertainties. Though that would lead one to assume that the two layers of cells had mixed before measurement, the consistent difference in shimming makes it less likely that they were completely mixed. Still, some mixing of the layers could contribute to the small differences in cell size and the large cell sizes in these measurements.

There was also no difference between the initial diffusion coefficients in the two layers. This was expected, because of the assumption that previous growth in initial diffusion was caused by changes in the apparent cell size and time dependent diffusion coefficients.

Next follows the plots of measured diffusion against the square root of diffusion time for the IC water signal.
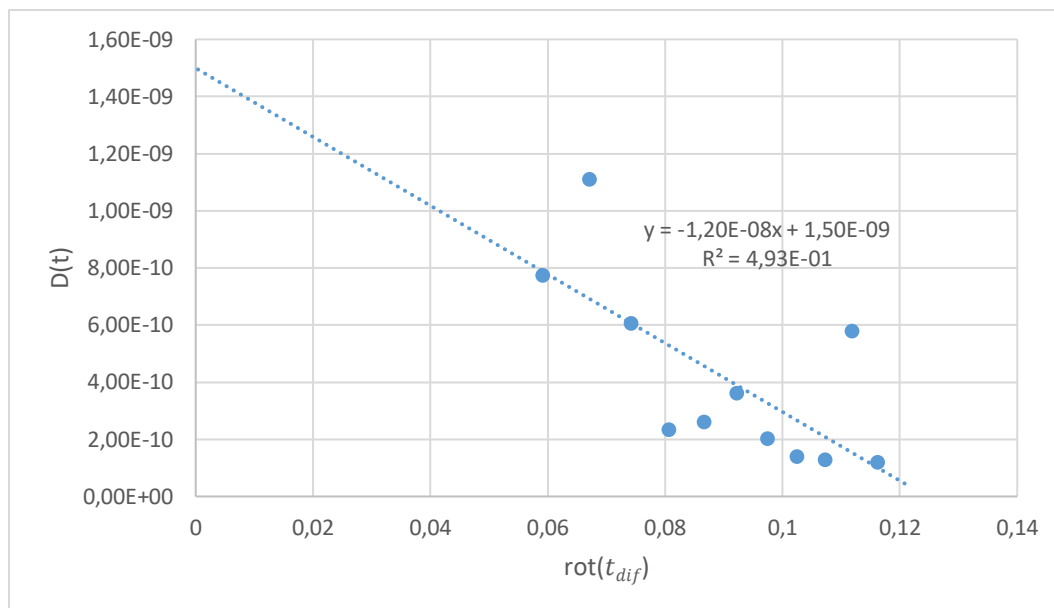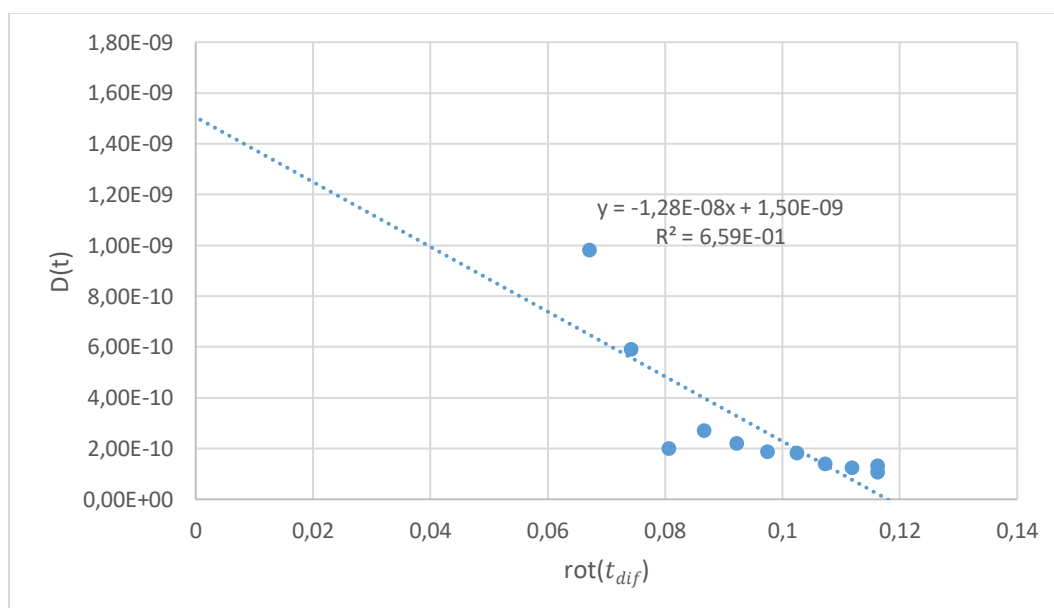
Figure 4.7.4 D(t) plotted against $\sqrt{t_{dif}}$ for the intracellular component of the water in the 26.08.19 slice selective diffusion measurements of a yeast cell suspension 3 mm below center, with the 12 day old suspension. Using equation 2.5.2 and 2.5.3 gives a cell radius of $4*10^{-6}$ $\pm1*10^{-6}$ m and an initial diffusion of $1,5*10^{-9}$ $\pm4*10^{-10}$ m^2/s. A repetition of the experiment gave the same cell radius of $4*10^{-6}$ $\pm1*10^{-6}$ m and an initial diffusion of $1,6*10^{-9}$ $\pm3*10^{-10}$ m^2/s.

Figure 4.7.5 D(t) plotted against $\sqrt{t_{dif}}$ for the intracellular component of the water in the 26.08.19 slice selective diffusion measurements of a yeast cell suspension 3 mm above center, with the 3 day old suspension. Using equation 2.5.2 and 2.5.3 gives a cell radius of $3,4*10^{-6}$ $\pm8*10^{-7}$ m and an initial diffusion of $1,5*10^{-9}$ $\pm3*10^{-10}$ m^2/s. A repetition of the experiment gave a cell radius of $3,8*10^{-6}$ $\pm8*10^{-7}$ m and an initial diffusion of $1,9*10^{-9}$ $\pm3*10^{-10}$ m^2/s.

In this case, as opposed to the non-selective measurements, there is an increase in the radius measured by the water signal, though it is also small enough to be within the uncertainties. The

water signal is seemingly also affected by what caused the apparent cell size of the Lysine signal to increase.

These measurements also had large uncertainties, similar to the ones in the Lysine signal measurements. This is a change from the non-selective measurements, where the water signal had particularly small uncertainties. This difference likely comes from some combination of the differing equipment, the different geometry of the sampled area, and the different method of measuring.

The water signal also shows larger initial diffusions as compared to the previous section, and by a much larger factor than the Lysine diffusion, around 10. It is difficult to determine what caused this, but it is possible that the gradient being weaker than calibrated for affected the water signal more. If this is the case, it could be because the gradient also would influence the EC water, and this could interfere with the IC component in some way.

5 Conclusions

5.1 Conclusions

This method for measuring the radius of cells in a yeast model system seems to give radii that are in line with other studies found in the literature, on the smaller end of the spectrum. The initial diffusion coefficients that were found for the different metabolites mostly follow the trend of the heavier metabolites having lower diffusion coefficients. The numbers found also seems to have reasonably low uncertainties.

The metabolite measurements of cell sizes in these yeast samples show apparent growth from around 1,9 µm at 3 days suspeded to around 3,5 µm at 12 days suspended. A comparison of spectrums from older and newer cells shows that there are changes in the metabolite signals. The apparent growth may come from the cell swelling or from the cell dying and having increased cell permeability.

The same growth is not apparent in the measurements of cell size based on the water signal, which stayed around 1,6 µm. That lack of apparent growth is likely a result of the water signal being less sensitive to microstructural changes in the yeast cell suspensions. This might be due to influence from the extracellular water signal, since water has a lot of EC water signal while the metabolites have virtually no EC signal. Another possible reason for the lack of sensitivity to microstructural changes is that there is less relative change in cell membrane permeability, as water already had comparatively rapid cell membrane exchange, as compared to the metabolites.

There is also apparent growth in the initial diffusion coefficient, which probably comes from an imperfect extrapolation, where the changes in time dependent diffusion coefficients also affected the initial diffusion. If the apparent growth in cell size is caused by swelling in the cells, then the increase in apparent initial diffusion could be due to changes in IC density.

The test for whether a metabolite in a 3 days old suspension had an EC component seemed to conclude that the metabolite did not seem to have an EC component. This was because the changes observed were too small, and the slower component solved for had to low of a diffusion coefficient to be the IC component.

The method of metabolite extraction used in this study, adapted from Alrodi et.al, gave an extract that measured as containing most of the metabolites that where identified in the Alrodi et.al study. Many signals could be identified as coming from certain metabolites, but overlap between signals prevented another large portion of signals from being identified. It may be easier to identify the metabolites when the yeast is grown as opposed to dried and resuspended, as that allows for separation of an exponential and a stationary phase, which makes the metabolite signals more easily identifiable.

The slice selective diffusion measurements gave cell sizes that were larger than the cell sizes from the non-selective measurements, around 4 µm and with larger uncertainties. The exact reason for the change in cell size is unknown, but it may be that a gradient was not calibrated correctly at the location that was measured. The larger uncertainties was likely from equipment of lower quality or the measurements having different geometry.

5.2 Further work

There are many ways this work could be improved. Chief among them are more cell size measurements, especially at different lengths of suspension. Such measurements would give a clearer picture of how the cell size develops, and could solidify the trends seen here. It would show at what point the apparent growth in cell size stops, as well as whether it speeds up or slows down. More measurement of different metabolite signals could also help to solidify trends.

To determine the accuracy of the cell size measurements it would be useful to use another, non-NMR method, to determine the yeast cell sizes. This could reveal whether there were any systematic errors in the cell size measurements.

It could also be interesting to look at yeast that is genetically modified to have larger cell sizes, to see whether the method used in this study could detect the change in cell size.

Another relevant test that could be performed is a repetition of the test for EC component of metabolites. Firstly, measuring more metabolites could be interesting, to see if any of them have an EC component. What could also be interesting is a similar test for an older yeast suspension. If the cell membrane dissolving was the reason for the apparent cell growth, the metabolites would be more likely to have an EC component in the older yeast suspensions.

As for the slice selective measurements, calibrating the gradient could make the results more in line with the non-slice selective results, if that was the actual cause of the potential error. Simply doing slice selective measurements in the middle of the sample, where the gradient would calibrated correctly, could also illuminate the source of the difference in cell size between selective and non-slice selective measurements. Measuring more slices could reveal to what degree the old and new yeast layers had mixed. Measuring a sample without layers on the same equipment could reveal any faults there, and measuring such a sample without slice selection could reveal whether the slice selective method was the source of the differences.

6 Sources

1. Martin, E.; "Oxford concise medical dictionary (9 ed.)"; **2015**
2. Sherman, F.; "Getting started with yeast"; **2002**
3. Bloch, F.; Hansen, W. W.; Packard, M.; *Nuclear induction*; Phys. Rev.; 69(3-4): 127-127, **1946**
4. Purcell, E.M.; Torrey, H.C.; Pound, R. V.; *Resonance absorption by nuclear magnetic moments in a solid*; Phys. Rev.; 69(1-2):37–38; **1946**.
5. Helmer, K. G.; Dardzinski B. J.; Sotak C. H.; *The Application of Porus-Media Theory to the Investigation of Time-Dependent Diffusion in In Vivo Systems;* NMR in Biomedicine; vol. 8, 297-306; **1995**
6. Mitra , P. P.; Sen, P. N.; Schwartz, L. M.; Le Doussal, P.; *Diffusion propagator as a probe of the structure of porous media*; Phys. Rev., Vol. 68 No. 24; **1992**
7. Mitra , P. P.; Sen, P. N.; Schwartz, L. M.; *Short-time behavior of the diffusion coefficient as a geometrical probe of porous media*; Phys. Rev., Vol. 47 No. 14; **1993**
8. Hürlimann, M. D.; Latour, L. L.; Sotak C. H.; *Diffusion Measurement in Sandstone Core: NMR Determination of Surface-to-Volume Ratio and Surface Relaxivity*; Magnetic Resonance Imaging, Vol. 12, No. 2, 325-327, **1994**
9. Latour, L. L.; Svoboda, K.; Mitra, P. P.; Sotak, C. H.; *Time-dependent diffusion of water in a biolocical model system,* Proc. Natl. Acad. Sci. USA Vol. 91; 1229-1233, **1994**
10. Ronen, I.; Valette, J.; *Diffusion-Weighted Magnetic Resconance Spectroscopy*; eMagRes; Vol 4:733-750; **2015**
11. Eriksson S.; Elbing, K.; Söderman, O.; Lindkvist-Peterson, K.; Topgaard, D.; Lasic S.; *NMR quantification of diffusional exchange in cell suspensions with relaxation rate diffrences between intra and extracellular compartments*, PLoS ONE 12(5) **2017**
12. Åslund, I.; Nowacka, A.; Nilsson, M.; Topgaard, D.; *Filter-Exchange PGSE NMR determination of cell membrane permability*; J. Magn. Reson. 200; 291–295; **2009**
13. Silva, M. D.; Helmer, K. G.; Lee, J.; Han, S. S.; Springer, C. S. Jr.; Sotak, C. H.; *Deconvolution of Compartmental Water Diffusion Coefficients in Yeast-Cell Suspensions Using Combined T_1 and Diffusion Measuremetns*; J. Magn. Reson. 156; 52–63 **2002**
14. Airoldi, C.; Tripodi, F.; Guzzi, C.; Nicastro, R.; Coccetti, P.; *NMR analysis of budding yeast metabolomics: a rapid method for sample preparation;* Mol. BioSyst.; 11, 379; **2015**
15. Keeler, J.; "Understanding NMR spectroscopy"; John Wiley & Sons, 2nd edition; **2011**
16. Gunther, H.; NMR Spectroscopy Basic Principles, Concepts and Applications in Chemistry; **2013**
17. Friebolin, H.; Becconsall, J. K., "Basic one-and two-dimensional NMR spectroscopy" VCH Weinheim: **1993**
18. Kontogeorgis, G. M.; Soren, K.; «Introduction to Applied Colloid and Surface Chemistry»; **2016**
19. Reiss, E.; Shadomy, H. J.; Lyon, G. M.; "Fundemental Medical Mycology"; **2012**
20. Sørland, H. G.; "Dynamic Pulse Field Gradient NMR"; **2014**
21. Brown, M. A.; Semelka, R. C.; "MRI Basic Principles and Applications"; **2003**
22. Hahn, E. L.; *Spin Echoes*; Phys. Rev.; 80(4):580; **1950**
23. Stejskal, E. O.; Tanner, J.E.; *Spin diffusion measurement: Spin echoes in the precence of a time-dependent field gradient*; J. Chem. Phys.; 42(1): 288-292; **1965**
24. Lewis, R. T.; "Characteriszing liqiuid dynamics and surface interactions in porous materials using Nuclear Magnetic Resonance", **2015**

25. Bernstein, M. A.; King, K. F.; Zhou, X. J.; "Handbook of MRI pulse sequences. Elsevier" 2004
26. Freeman, R; *Shaped radiofrequency pulses in high resolution nmr*; Prog. Nucl. Magn. Reson. Spectrosc., 32(1):59–106, **1998**
27. Berger, S,; *Nmr techniques employing selective radiofrequency pulses in combination with pulsed field gradients*; Prog. Nucl. Magn. Reson. Spectrosc.; 30(3-4):137–156, **1997**
28. Hoult, D. I.; *Solvent peak saturation with single phase and quadrature fourier transform;* J. Magn. Reson.; **1976**
29. Zheng, G.; Price, W.S.; *Solvent signal suppression in nmr;* Prog. Nucl. Magn. Reson. Spectrosc., 56(3) 267-288; **2010**
30. Zamir, D.; Wayne, R.C.; Cotts, R.M.; *Anomalous nuclear magnetic resonance linewidth in lithium;* Phys. Rev. Lett., 12(12):327–330, **1964**
31. Cotts, R. M.; Hoch, M. J. R.; Sun, T.; Markert, J. T.; *Pulsed field gradient stimulated echo methods for improved nmr diffusion measurements in heterogeneous systems*; J. Magn. Reson., 83(2):252 – 266, **1989**
32. Wisniewska, M. A.; "Characterizing mass transport in hydrogels using Nuclear Magnetic Resonance"; PhD thesis; **2019**
33. Svenkrtova, A.; Belicova, L.; Volejnikova, A.; Sigler, K.; Jazwinski, S. M.; Pichova, A.; *Stratification of yeast cells during chronological aging by size points to the role of Trehalose in cell vitality*; Biogerontology; **2016**
34. Helmer, K. G.; Hürlimann, M. D.; De Swiet, T. M.; Sen, P. N.; Sotak C. H.; *Determination of Ratio of Surface Area to Pore Volume from Restricted Diffusion in a Constant Field Gradient*, **1994**
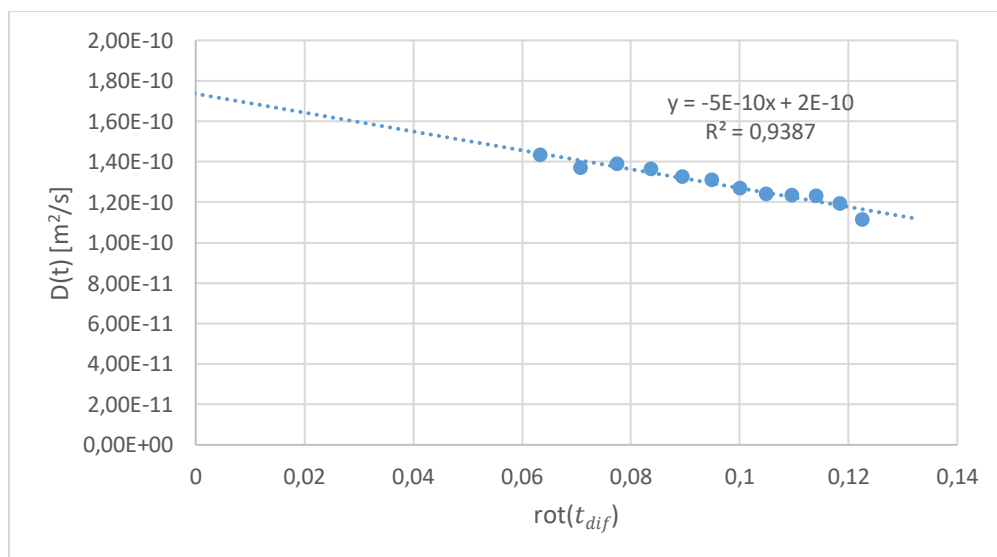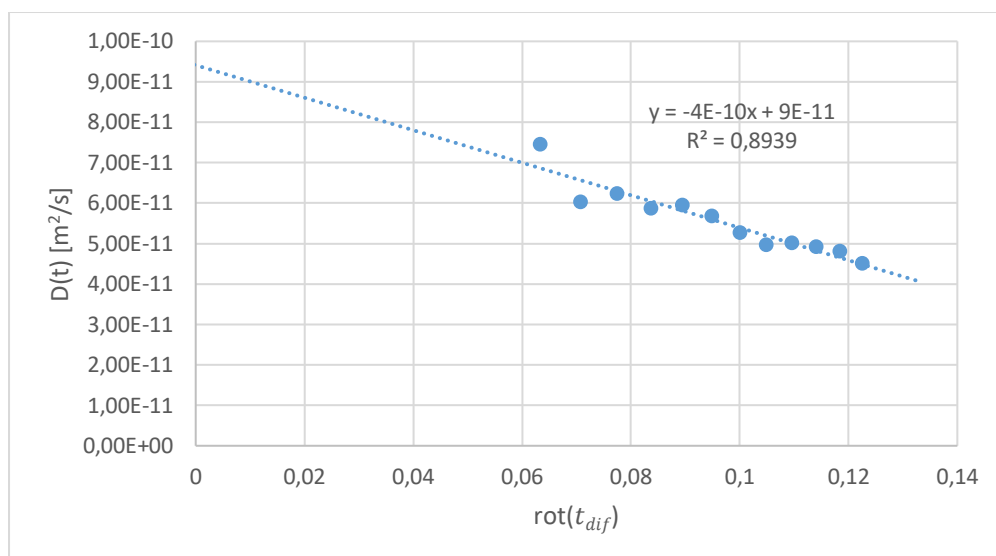
Appendix

A)
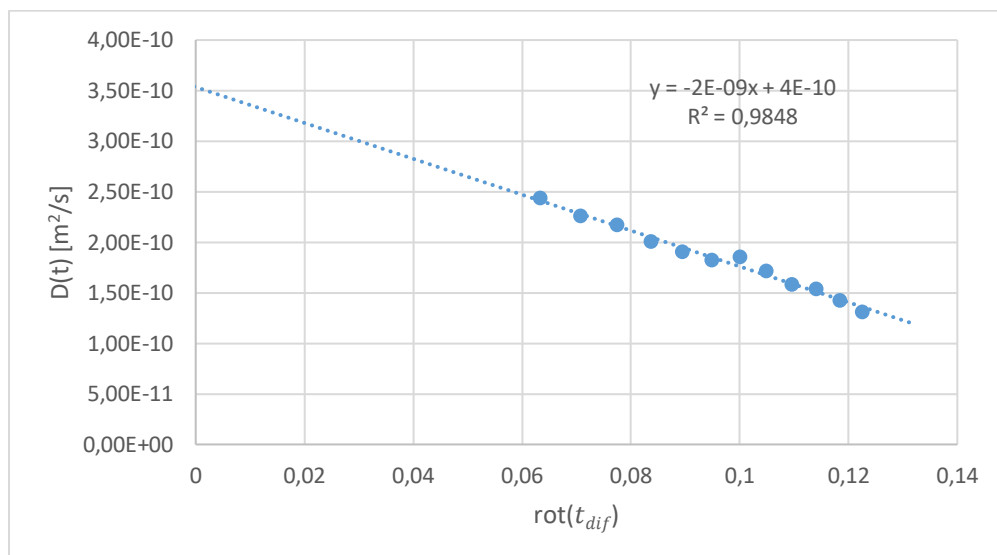
B)

Figure A1: D(t) plotted against $\sqrt{t_{dif}}$ for the Trehalose signal at 3,4 ppm in the diffusion measurements of A) sample 1 and B) sample 5.
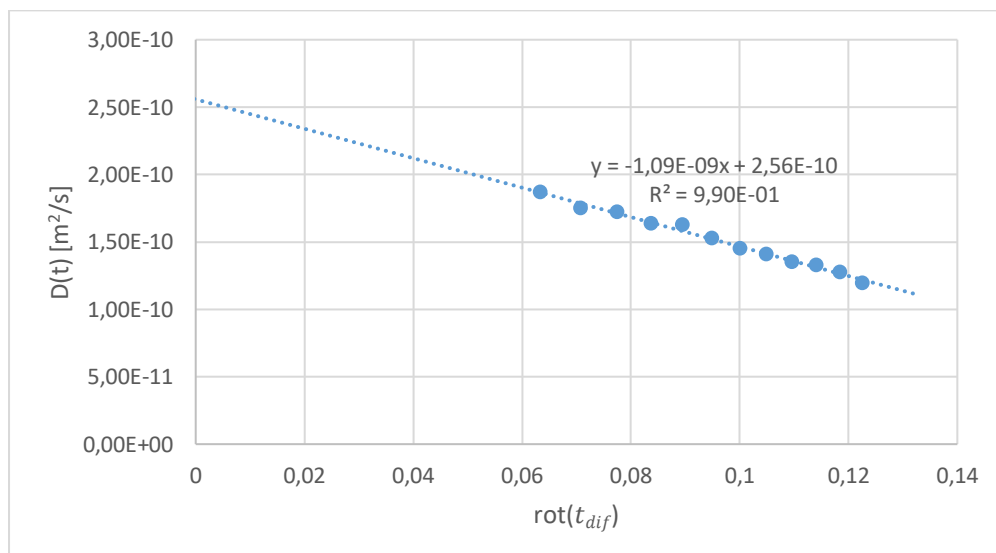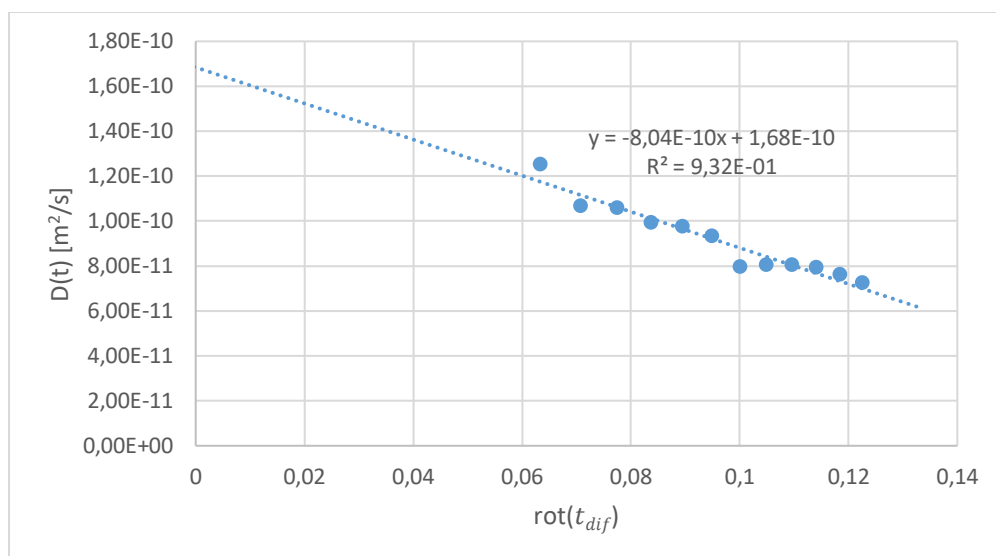
A)

B)

Figure A2: D(t) plotted against $\sqrt{t_{dif}}$ for the Glycerophosphocholine signal at 3,2 ppm in the diffusion measurements of A) sample 1 and B) sample 5.
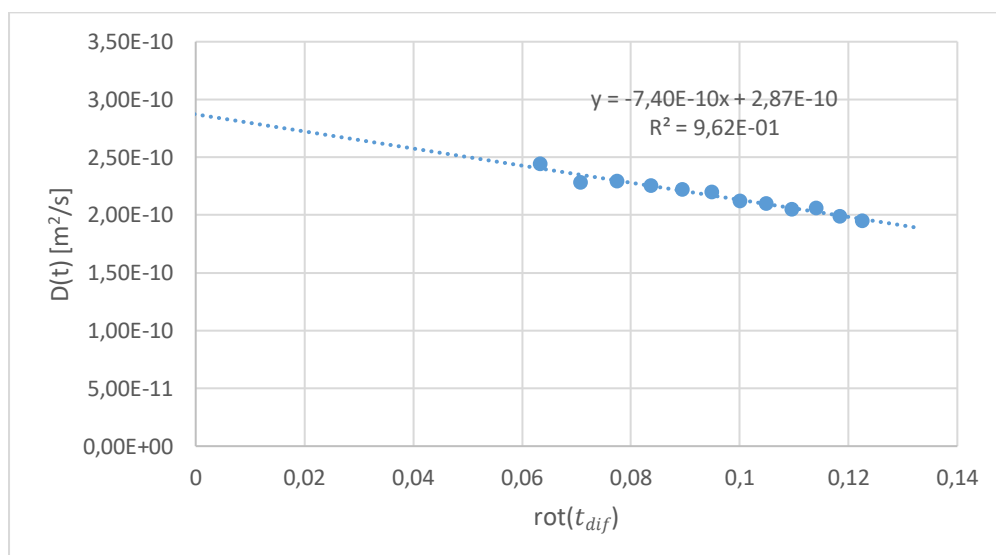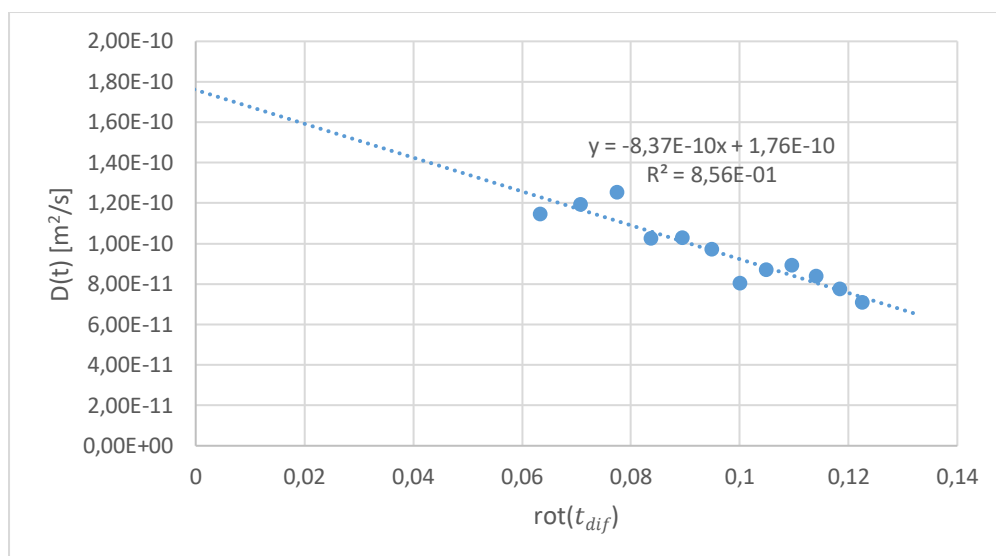
A)

B)

Figure A3: D(t) plotted against $\sqrt{t_{dif}}$ for the Lysine signal at 3 ppm in the diffusion measurements of A) sample 1 and B) sample 5.
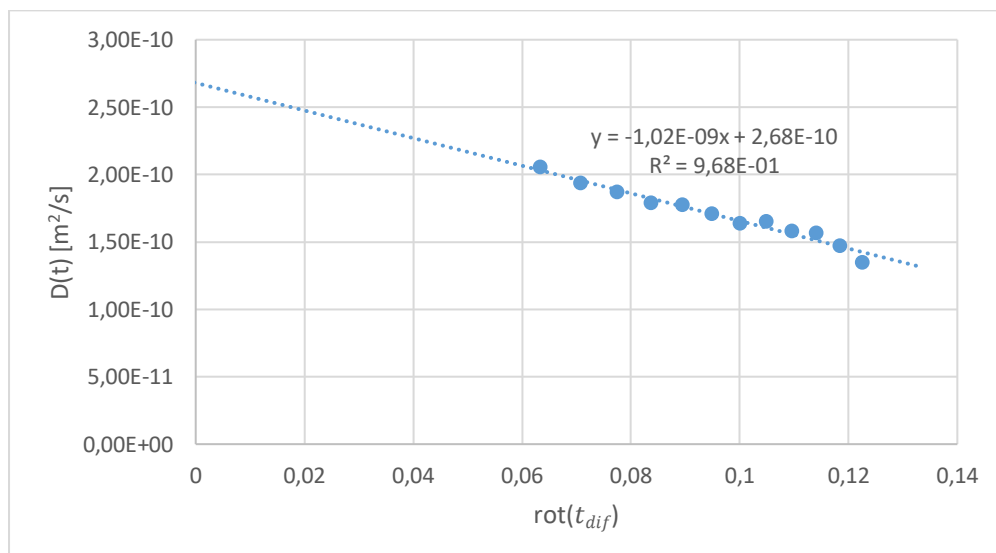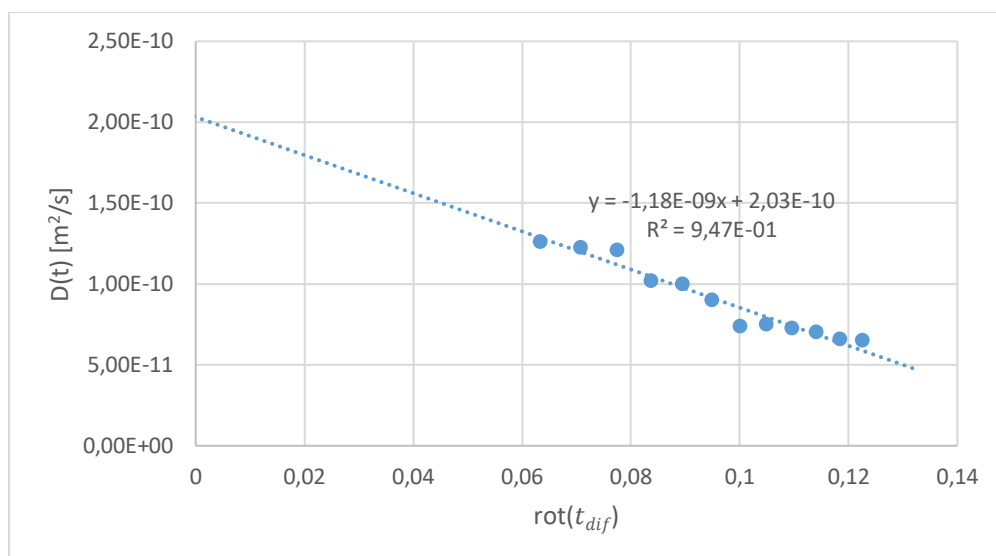
A)

B)

Figure A4: D(t) plotted against $\sqrt{t_{dif}}$ for the Lysine signal at 1,7 ppm in the diffusion measurements of A) sample 1 and B) sample 5.
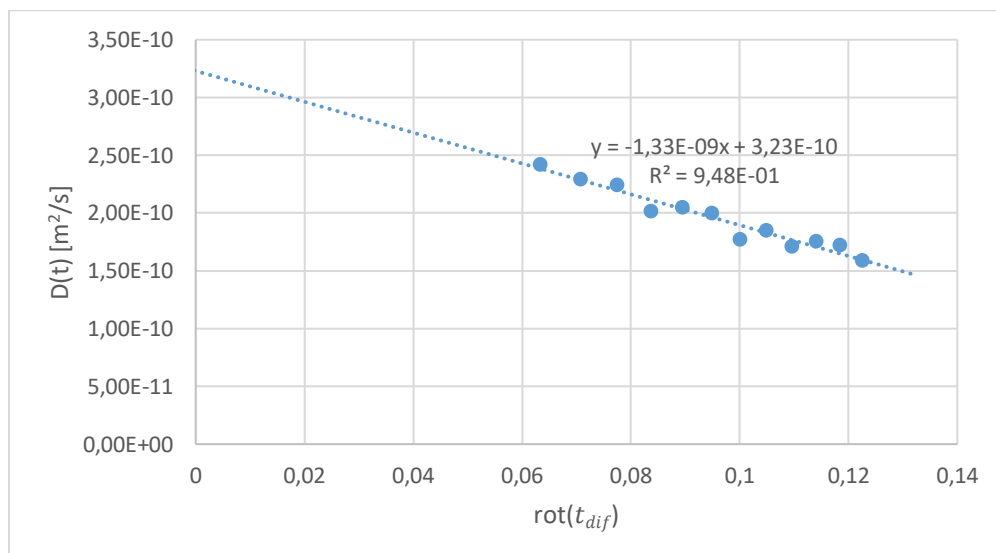
A)

B)

Figure A5: D(t) plotted against $\sqrt{t_{dif}}$ for the Lysine signal at 1,47 ppm in the diffusion measurements of A) sample 1 and B) sample 5.